OLIGO(ETHYLENE GLYCOL) CHAINS: APPLICATIONS AND ADVANCEMENTS IN BIOSENSING

A Thesis
Presented to
The Academic Faculty

by

Jonathan J. Bryant

In Partial Fulfillment
of the Requirements for the Degree
Master of Science in the
School of Chemistry and Biochemistry

Georgia Institute of Technology
December 2010

OLIGO(ETHYLENE GLYCOL) CHAINS: APPLICATIONS AND ADVANCEMENTS IN BIOSENSING

Approved by:

Dr. Uwe Bunz, Advisor
School of Chemistry and Biochemistry
Georgia Institute of Technology

Dr. David Collard
School of Chemistry and Biochemistry
Georgia Institute of Technology

Dr. Stefan France
School of Chemistry and Biochemistry
Georgia Institute of Technology

Date Approved: September 29, 2010

ACKNOWLEDGEMENTS

I would like to thank my advisor, Prof. Uwe Bunz, for providing employment and opportunity. Also, thanks to everyone in the Bunz lab, past and present, for their advice and help, particularly Anthony Zucchero, Juan Tolosa, Evan Davey, and Ronnie Phillips.

TABLE OF CONTENTS

	Page
ACKNOWLEDGEMENTS	iii
LIST OF FIGURES	v
SUMMARY	viii
CHAPTER	
1 Introduction	1
Conjugated Polymers as Biosensing Platforms	1
Poly(*para*-phenyleneethynylene)s as Biosensors	3
2 Swallowtail Polymers for Biosensing	8
Introduction	8
Constructing a Polymer Array for Glycan Biosensing	8
A Red-Emissive Water-Soluble PPE	13
Conclusions	14
Experimental	14
3 Plasmonic Field Enhancement of an Ampiphilic Fluorescent Polymer	19
Introduction	19
Discussion	21
Conclusions	24
Experimental	24
APPENDIX A: Synthesis of Diiododihydroquinone	28
APPENDIX B: NMR Spectra	29
REFERENCES	45

LIST OF FIGURES

		Page
Figure 1.1:	Representation of Bazan's DNA sensor	3
Figure 1.2:	Fluorescence microscopy images of cancer cells after staining with PPE; transmittance images (left) and fluorescence images (right).	4
Figure 1.3:	Quenching of a sugar-substituted PPE by concanavalin A	5
Figure 1.4:	Depiction of PPE/NP construct as a turn-on sensor for bacteria	5
Figure 1.5:	Plot for the first three factors of simplified fluorescence response patterns obtained with PPE array against 17 protein analytes	6
Figure 2.1:	Polymers used in biosensing array	10
Figure 2.2:	Synthesis of PPE **2b**	10
Figure 2.3:	Normalized absorption (red, blue, and green) and emission (orange, yellow, and purple) spectra of PPEs **2.7**, **2.8**, and **2b**	11
Figure 2.4:	Synthesis of monomer **2.6**	12
Figure 2.5:	Water-soluble PPE-PPV hybrid	13
Figure 3.1:	PPE **3**	19
Figure 3.2:	(A) Fluoresence spectra of PPE monolayer deposited on silver nanocubes as a function of nanocube surface density. (B) Integrated fluorescent intensity as a function of nanocube surface density.	20
Figure 3.3:	Synthetic scheme for PPE **3**	21
Figure 3.4:	Normalized absorption (red and blue) and emission (green and yellow) spectra of PPEs **3.6** and **3.7** in $CHCl_3$	22
Figure 3.5:	Normalized absorption (red, blue, and green) and emission (orange, yellow, and purple) spectra of PPEs **3** in H_2O	22
Figure 3.6:	Synthetic scheme for monomer **3.5**	23
Figure B.1:	^1H NMR spectrum of **2.1** and **3.1** in $CDCl_3$	29
Figure B.2:	^{13}C NMR spectrum of **2.1** and **3.1** in $CDCl_3$	29
Figure B.3:	^1H NMR spectrum of **2.2** in $CDCl_3$	30

Figure B.4: ^{13}C NMR spectrum of **2.2** in $CDCl_3$ 30

Figure B.5: ^{1}H NMR spectrum of **2.3** in $CDCl_3$ 31

Figure B.6: ^{13}C NMR spectrum of **2.3** in $CDCl_3$ 31

Figure B.7: ^{1}H NMR spectrum of **2.4** in $CDCl_3$ 32

Figure B.8: ^{13}C NMR spectrum of **2.4** in $CDCl_3$ 32

Figure B.9: ^{1}H NMR spectrum of **2.5** in $CDCl_3$ 33

Figure B.10: ^{13}C NMR spectrum of **2.5** in $CDCl_3$ 33

Figure B.11: ^{1}H NMR spectrum of **2.6** in $CDCl_3$ 34

Figure B.12: ^{13}C NMR spectrum of **2.6** in $CDCl_3$ 34

Figure B.13: ^{1}H NMR spectrum of **2.7** in $CDCl_3$ 35

Figure B.14: ^{13}C NMR spectrum of **2.7** in $CDCl_3$ 35

Figure B.15: ^{1}H NMR spectrum of **3.2** in $CDCl_3$ 36

Figure B.16: ^{13}C NMR spectrum of **3.2** in $CDCl_3$ 36

Figure B.17: ^{1}H NMR spectrum of **3.3** in $CDCl_3$ 37

Figure B.18: ^{13}C NMR spectrum of **3.3** in $CDCl_3$ 37

Figure B.19: ^{1}H NMR spectrum of **3.4** in $CDCl_3$ 38

Figure B.20: ^{13}C NMR spectrum of **3.4** in $CDCl_3$ 38

Figure B.21: ^{1}H NMR spectrum of **3.5** in $CDCl_3$ 39

Figure B.22: ^{13}C NMR spectrum of **3.5** in $CDCl_3$ 39

Figure B.23: ^{1}H NMR spectrum of **3.6** in $CDCl_3$ 40

Figure B.24: ^{13}C NMR spectrum of **3.6** in $CDCl_3$ 40

Figure B.25: ^{1}H NMR spectrum of **3.7** in $CDCl_3$ 41

Figure B.26: ^{1}H NMR spectrum of **3** in D_2O 41

Figure B.27: ^{1}H NMR spectrum of **3** in DMSO 42

Figure B.28: ^{1}H NMR spectrum of 2,5-diiiodo(*p*-dimethoxybenzene) in $CDCl_3$ 42

Figure B.29: ^{13}C NMR spectrum of 2,5-diiodo(*p*-dimethoxybenzene) in $CDCl_3$ 43

Figure B.30: ^{1}H NMR spectrum of 2,5-diiododihyroquinone in $CDCl_3$ 43

Figure B.31: ^{13}C NMR spectrum of 2,5-diiododihydroquinone in DMSO 44

SUMMARY

Oligo(ethylene glycol) groups have been used as substituents in poly(*p*-phenyleneethynylene)s (PPEs) to provide solubility, and to boost quantum yield. Properties such as water-solubility and increased quantum yield in aqueous solution make these conjugated systems promising for biosensory applications.

In this thesis, a PPE containing a branched ethylene glycol side chain is synthesized as part of a polymer array for glycan biosensing. I also report that the same side chain can be put to use in a red-emissive polymer to lend water solubility. Another monomeric unit, containing ethylene glycol chains, is incorporated into a PPE to create an ampiphilic polymer. The versatility of these polymers allows them to be used for a variety of purposes, some of which will be described herein.

CHAPTER 1

INTRODUCTION

1.1 Conjugated Polymers as Biosensing Platforms

Conjugated polymers (CPs) have long been known as electronic materials;[1] those that are fluorescent are also of interest as sensory materials.[2] These fluorescent polymers have sparked interest in the field of chemical sensing due to their ability to produce a measurable signal response upon interaction with a variety of analytes. The response of CPs being more sensitive than that of traditional fluorescent dyes has led to them being referred to as amplifying fluorescent polymers.[3] Amplification of the fluorescent signal of a CP in response to an analyte is due to the polymer acting as a "molecular wire."[4] As opposed to a small molecule, the fluorescence of which is quenched by an analyte within a certain radius, the fluorescence of a conjugated polymer can be quenched at any point along the polymer backbone due to exciton migration.[3, 5] Typical fluorescent lifetimes are long enough that the exciton is able to travel up to 100 repeat units before fluorescing, interacting with any quenching species anywhere along that chain. These fluorescent compounds have been used in a myriad of sensing schemes, from detection of explosives[6] and volatile organic compounds,[7] to metal sensing.[8] These sensory techniques can be extended to the field of biosensing by synthesizing CPs that are soluble in water.[9] Often these hydrophilic polymers are realized by using pendant ionic substituents.[4] Sulfonate, phosphonate, and carboxylate side chains provide negatively charged water-soluble polymers. Side chains with quaternary amine groups provide cationic polymers. A wide variety of sensing schemes, relying on the fluorescent response of water-soluble CPs, have enabled the detection of biological species such as DNA,[10] proteins,[11] bacteria,[12] and glucose.[13]

One simple detection method is to fluorescently label the target analyte. This can be done by designing a polymer with side chains that have an affinity for that certain analyte. Disney, *et al*., used a polymer with mannose side chains to stain bacteria with mannose receptors on the cell surface.[12] A more common strategy is to measure the fluorescent response of the polymer. This response can be a hypsochromic or bathochromic shift in the absorption or emission, or a change in the fluorescent intensity (quenching), or both. Gaylord and coworkers developed a novel sensor able to detect single-stranded DNA (ssDNA).[10a] The sensor (Figure 1.1) utilizes the electrostatic interaction between a cationic fluorene-based copolymer and negatively charged DNA, and the fluorescence resonance energy transfer (FRET) between the polymer and a chromophore (fluorescein). The fluorescein is functionalized to a peptide nucleic acid (PNA) strand, and when mixed with the polymer, no FRET occurs. Only in the presence of a complementary strand of ssDNA is the fluorescein (F) then brought close enough to the polymer for FRET to occur, at which point the fluorescein will dominate the emission. The wavelength shift of the emission maximum due to FRET reveals the presence of a specific sequence of ssDNA.

Sensors can also be based on changes in fluorescent intensity. Generally, this involves some sort of quenching mechanism. Zhao and coworkers used a carboxylate-functionalized CP to detect pyrophosphate.[14] The polymer is first electrostatically bound to copper cations, which serve to quench the fluorescence of the system. In the presence of pyrophosphate, the copper binds preferentially to pyrophosphate, and the fluorescence of the system is restored. This is an example of a "turn-on" sensing scheme, as opposed to a "turn-off" system, where the analyte acts as a fluorescence quencher. Fan, *et al*., reported on the quenching of an anionic poly(*p*-phenylenevinylene) (PPV) by the protein cytochrome *c* via an electron transfer mechanism.[15] Other "turn-off" sensing schemes employ the self-quenching of the polymer.[11b, 16] Liu, *et al.*, examined quenching of their anionic poly(*p*-phenylene) derivative by positively-charged proteins and dendrimers. The

quenching was found to be based on conformational changes of the polymer as opposed to an energy or electron transfer mechanism.[16]

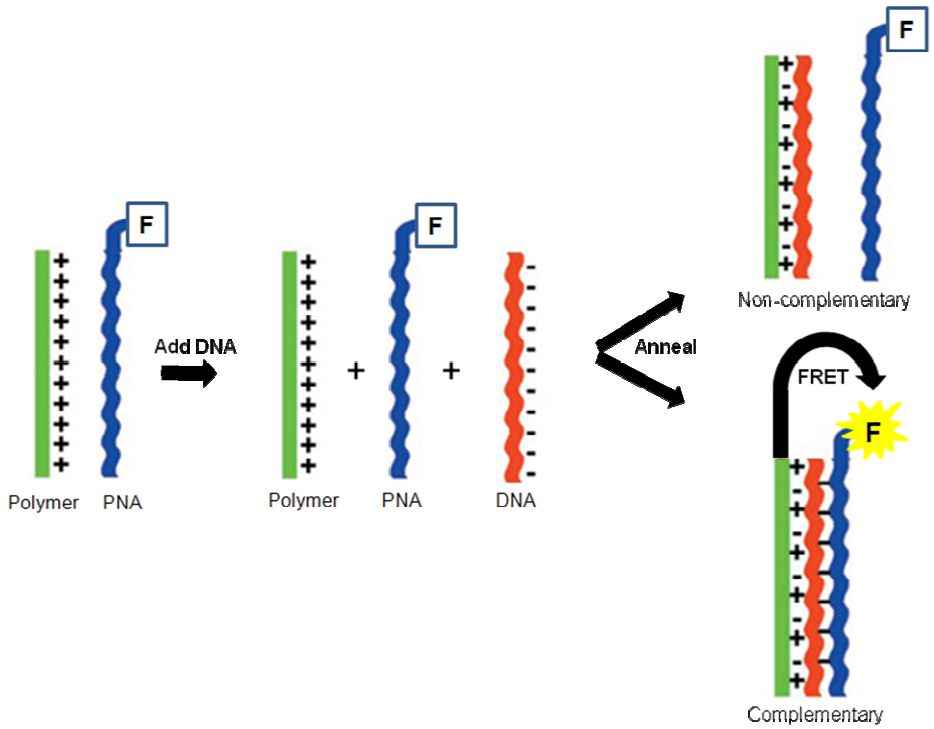

Figure 1.1 Representation of Bazan's DNA sensor[10a]

Another powerful sensing technique involves using polymer arrays. By combining different polymers with selectivity for a variety of analytes, a polymer sensor array is created. The components of the array are selective rather than specific, but when used in combination, an analyte-specific pattern can be generated.[17] Statistical software can be used to analyze the data, recognizing distinct individual patterns in response to an analyte. This array-based approach is analogous to olfactory systems,[18] hence the expression "chemical nose." Previous work in the Bunz group has explored the potential for sensing with polymer arrays, as well as implementing detection methods similar to the ones already discussed. In these experiments, the focus in the Bunz group has been on poly(*p*-phenylenethynylene)s (PPEs), which will be discussed in more detail.

1.2 Poly(*para*-phenyleneethynylene)s as Biosensors

PPEs are one class of fluorescent conjugated polymers, consisting of alternating phenylene and ethynylene groups. They have become popular for chemical sensing purposes due to their advantageous properties, including facile synthesis and versatile functionality, good quantum yield and photostability, and the dependence of their photophysical properties on their surrounding environment.[2] One of the attractive qualities offered by PPEs is their versatility. The fluorescent backbone of a PPE can be functionalized with a multitude of different side chains, introducing selectivity for a variety of analytes,[19] or providing solubility in different solvents[20], even altering the photophysical properties.[20-21] The extreme sensitivity offered by PPEs is another benefit. The quantum yield can be thought of as the efficiency of the polymer, or the percent of absorbed photons that are emitted as light. Certain dialkoxy-PPEs have shown quantum yields close to unity in dilute solutions.[2]

Experiments in the Bunz group have demonstrated the versatility of PPEs, from sensing of toxic, environmentally hazardous metal ions such as mercury[22] and lead,[23] to applications in biosensing. These sensing experiments have employed the same types of schemes already discussed. A folic acid functionalized PPE was used to stain and visualize cancer cells.[24]

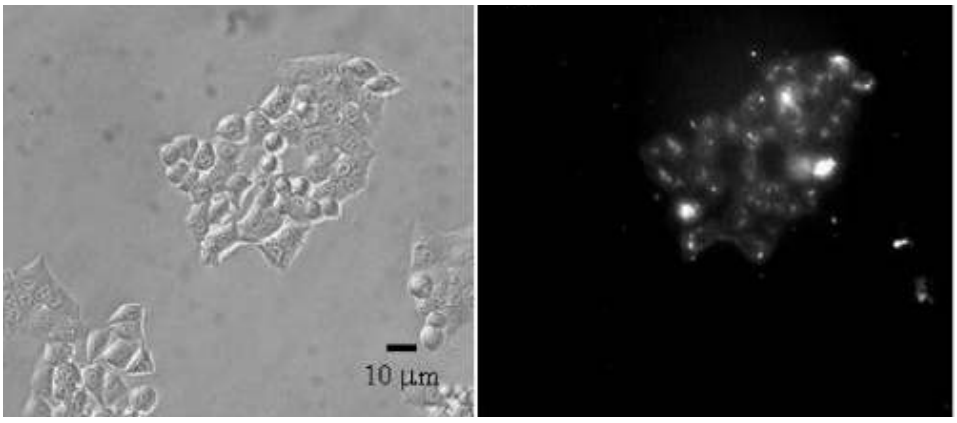

Figure 1.2 Fluorescence microscopy images of cancer cells after staining with PPE; Transmittance images (left) and fluorescence images (right).[24]

A "turn-off" sensor was developed to detect the lectin concanavalin A (Con A), by determining the quenching of the fluorescence of a mannose-substituted PPE upon binding (Figure 1.3).[19a]

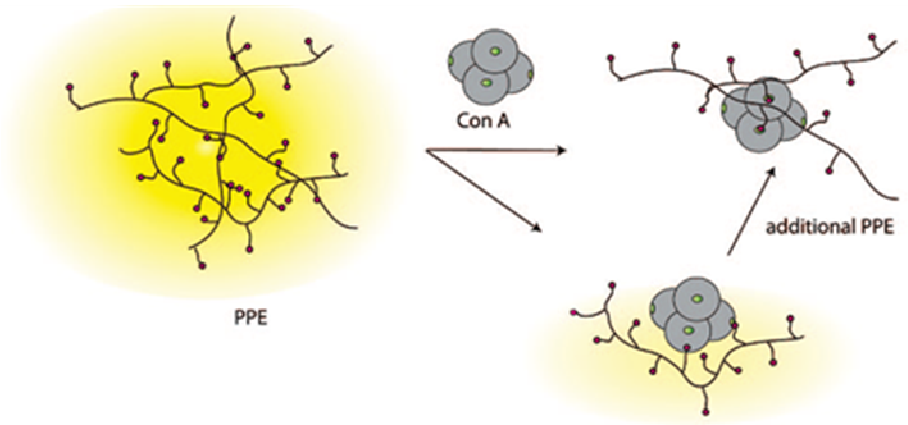

Figure 1.3 Quenching of a sugar-substituted PPE by concanavalin A[19a]

Figure 1.4 shows an example of a "turn-on" sensor for bacteria, involving PPEs that are electrostatically bound to gold nanoparticles (NPs). The fluorescence of the polymer is quenched by the NP in this system. Upon exposure to bacteria, the NPs preferentially bind to the cell surface, releasing the polymer, and restoring fluorescence. This system utilizes an array of different NPs to accurately discriminate between twelve strains of bacteria, including three different strains of *E. coli*.[25]

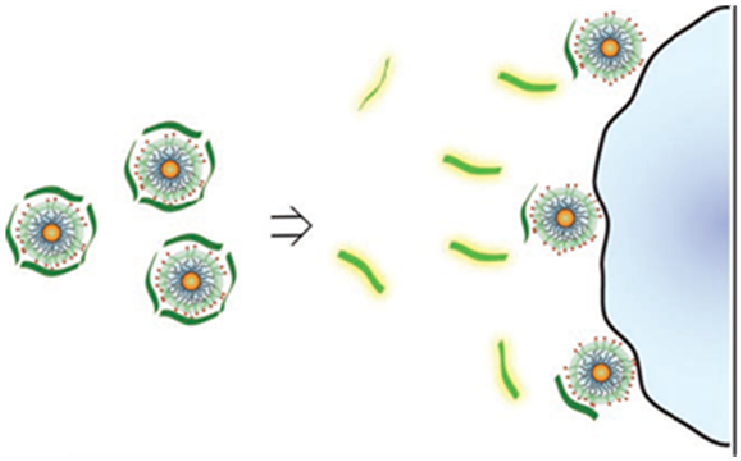

Figure 1.4 Depiction of PPE/NP construct as a turn-on sensor for bacteria[25]

The Bunz group has also utilized polymer arrays for biosensory applications. An array of six different PPEs has proven useful for differentiation of seventeen biological proteins.[26] Due to the unique interactions of each protein with each of the polymers, and the different effect seen on the fluorescence of each polymer, unique responses can be measured for the different proteins.

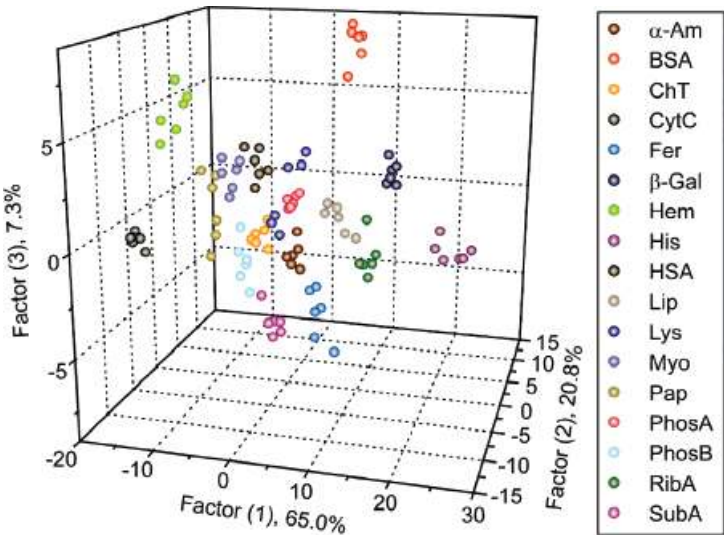

Figure 1.5 Plot for the first three factors of simplified fluorescence response patterns obtained with PPE polymer array against 17 protein analytes[26]

All of these biosensing experiments must be performed in an aqueous environment. For this to be possible, the sensing element must be soluble in water. Use of ionic side chains is a common route to solubilizing PPEs.[27] Ampiphilic oligo(ethylene glycol) moieties also provide solubility in a number of solvents, including water. One drawback is that the polymer species, while being soluble in water, tends to aggregate, thereby inducing self-quenching. Use of a branched oligo(ethylene glycol) side chain not only lends solubility, but has been shown to reduce aggregation, resulting in higher quantum yields,[20] which translates into higher sensitivity for biosensory applications. These types of functional groups continue to prove useful – in chemical sensing systems,

and in providing water-solubility to other organic systems. In this thesis, the following chapters detail the occurrence and use of ethylene glycol chains in conjugated polymers. Chapter 2 covers the use of a branched oligo(ethylene glycol), or "swallowtail" side chain in two different conjugated polymers. Chapter 3 examines the role of a triethylene glycol side chain as part of a conjugated polymer. In summary, the role that ethylene glycol chains play in these conjugated systems and the benefits of their use will be discussed.

CHAPTER 2

SWALLOWTAIL POLYMERS FOR BIOSENSING

2.1 Introduction

Building poly(*p*-phenyleneethynylene)s (PPEs) with ionic side chains is a common route for bringing them into aqueous environments. Quantum yields for ionic PPEs in water are generally low (Φ_f = 0.03-0.10).[5b, 20, 28] Hyperbranched conjugated polymers[29] and dendrimer-like side chains have recently been used to amplify quantum yields in aqueous solution.[30] Khan, *et al*., reported on the synthesis of a PPE bearing branched oligo(ethylene glycol), or "swallowtail" side chains.[20] Introduction of the swallowtail functionality furnished a water-soluble, chemically inert PPE with a high fluorescence quantum yield in water (Φ_f = 0.43). Addition of metal ions and variations in pH did not induce noticeable changes in the photophysical properties of the PPE.[20] Because of its high quantum yield and solubilizing properties, the swallowtail moiety has found use in the Bunz group as a substituent in certain copolymers.[21b, 25] This chapter highlights two such instances of the swallowtail and its use in PPEs.

2.2 Constructing a Polymer Array for Glycan Biosensing

2.2.1 Background

Glycans are oligo- or polysaccharides, and can be found either in free form, or bound to proteins or lipids (glycoconjugates).[31] Glycans can be found on the surface of cells, and it is well known that changes in glycosylation pattern are a trademark of cancer cells.[31-32] A wide range of cancers overexpress glycans, either on the cell surface, or by shedding them into the bloodstream. Though this phenomenon is found in all malignant tumors, different types will express their own specific glycosylation pattern.[33] Successful

identification of glycans, particularly the pattern on cell surfaces, could be instrumental in assigning the tumorigenic or non-tumorigenic nature of cells.[34]

Previous work by the Rotello group, in collaboration with the Bunz group, exploits an array based sensing approach for differentiation of normal, cancerous, and metastatic human breast cells.[35] The sensor array works based upon the physicochemical differences between cell surfaces. Following up this work, the Rotello group has recently developed a novel "chemical nose" sensor for glycans. An array of four different cationic poly(*p*-phenyleneethynylene)s (PPEs), each electrostatically bound to green fluorescent protein (GFP), are used as the sensory element. The fluorescence resonance energy transfer (FRET) between the two fluorescent species varies in response to different glycans. Using the array of polymer/GFP constructs, analyte-specific responses in the FRET can be measured. Experiments performed by Bajaj and coworkers show the efficacy of this system for detecting free glycans in solution, and differentiating between two different mammalian cell types (wild and mutant) based upon glycans present on the cell surface. The polymers comprising the array are a product of the Bunz lab; one in particular will be discussed further.

2.2.2 Discussion

The sensor array used in this experiment is composed of four polymers, shown in Figure 2.1, each electrostatically bound to GFP. Each of these distinct polymers must be (1) soluble in water, (2) positively charged, and (3) display FRET when coupled to GFP. The first two requirements can be met using positively charged amino groups, which are present in every polymer. The polymers display similar spectral properties; all of them exhibit FRET when coupled with GFP. Of the four polymers, **2d** is the least complex, while meeting all the requirements; the others are variations of this polymer. **2c** differs by varying the charge density. The copolymers **2a** and **2b** contain ethylene glycol side chains. The synthetic route to **2b** is shown in Figure 2.2. PPE **2.7** was prepared via

Sonogashira coupling of monomers **2.1** and **2.6**. Polymer **2.7** was then post-functionalized with *N*,*N*-dimethylethylenediamine to yield **2.7**. The quaternary amine was created with iodomethane to give **2b**.

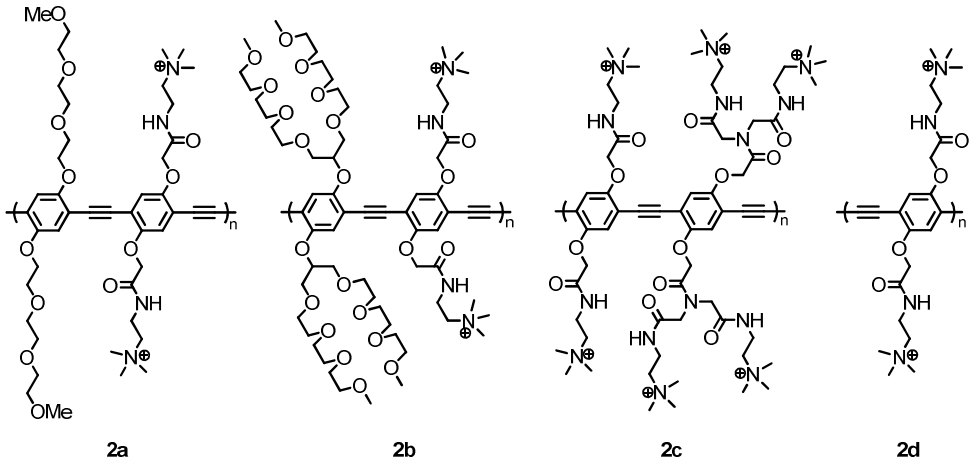

Figure 2.1 Polymers used in biosensing array

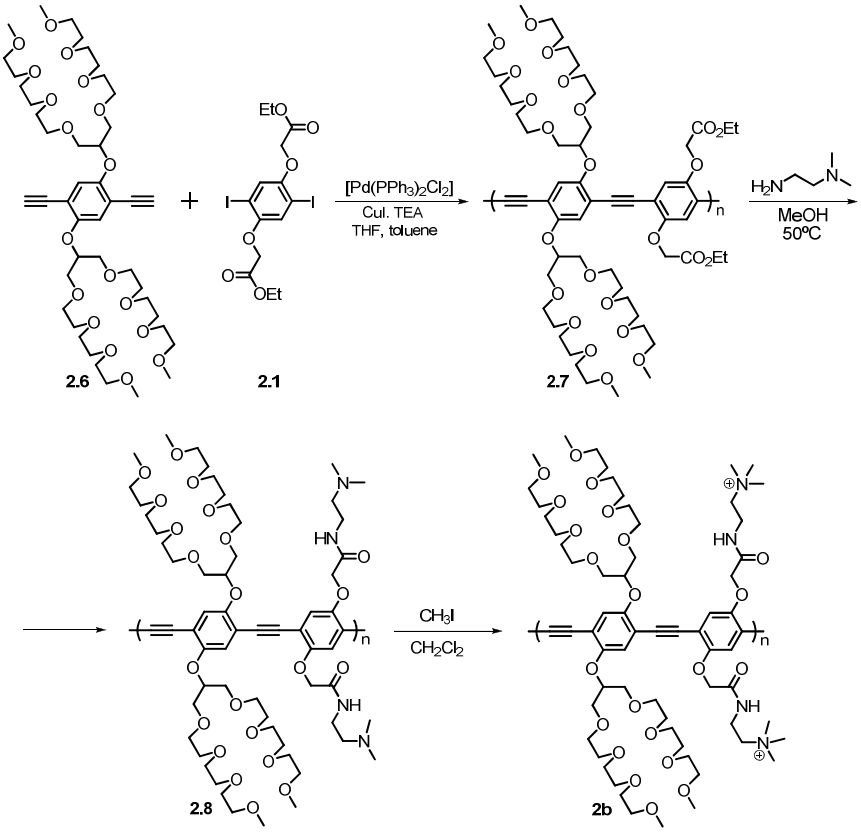

Figure 2.2 Synthesis of PPE **2b**

Incorporation of the swallowtail side chain into polymer **2b** serves to create a polymer that will interact with glycans differently than the others in the array. The combination of different responses from the four polymers enables the array to produce an overall response that is analyte-specific. Polymer **2b** also maintains the required solubility in water, and the photophysical properties are such that **2b** will exhibit FRET when coupled with GFP. Absorption and emission profiles of PPEs **2.7**, **2.8**, and **2b** are shown in Figure 2.2. The data for **2.7** and **2.8** were collected in $CHCl_3$; and for **2b** in H_2O.

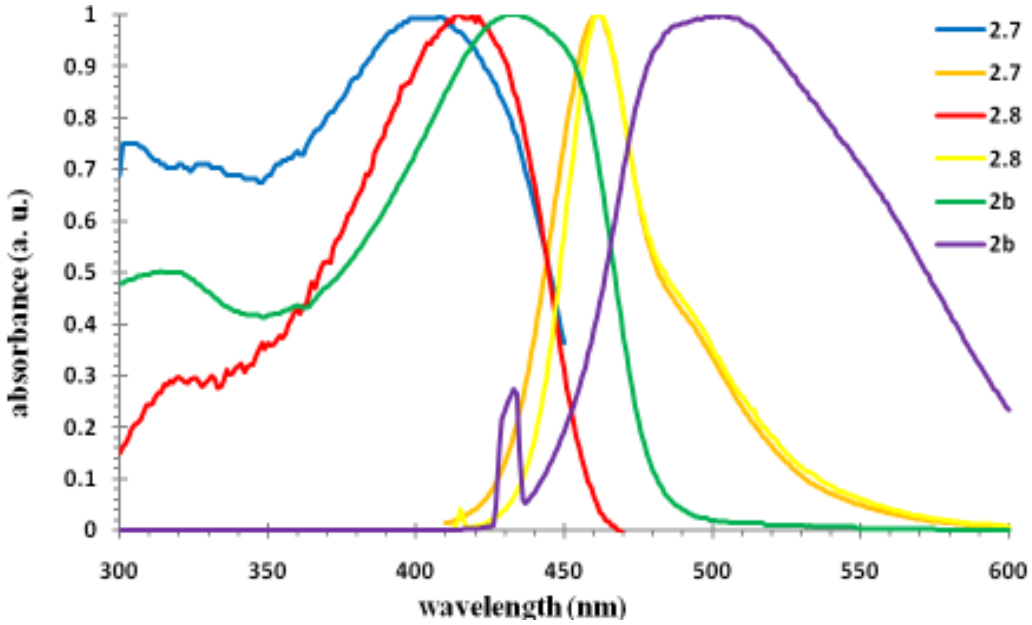

Figure 2.3 Normalized absorption (red, blue, and green) and emission (orange, yellow, and purple) spectra of PPEs **2.7**, **2.8**, and **2b**

Monomer **2.1** was synthesized by alkylation of 2,5-diiododihydroquinone with bromoethyl acetate. Monomer **2.6** was synthesized as shown in Figure 2.4. The swallowtail side chain was made by addition of tri(ethylene glycol) monomethyl ether to epichlorohydrin, yielding the alcohol **2.2**. Following tosylation, the side chain was added to the phenyl ring by alkylation of 2,5-diiododihydroquinone, producing the A_2 monomer **2.4**. The alkyne functionality was then introduced by Sonogashira coupling of

trimethylsilyl acetylene. Subsequent deprotection with potassium fluoride hydrate gave the B_2 monomer **2.6.**

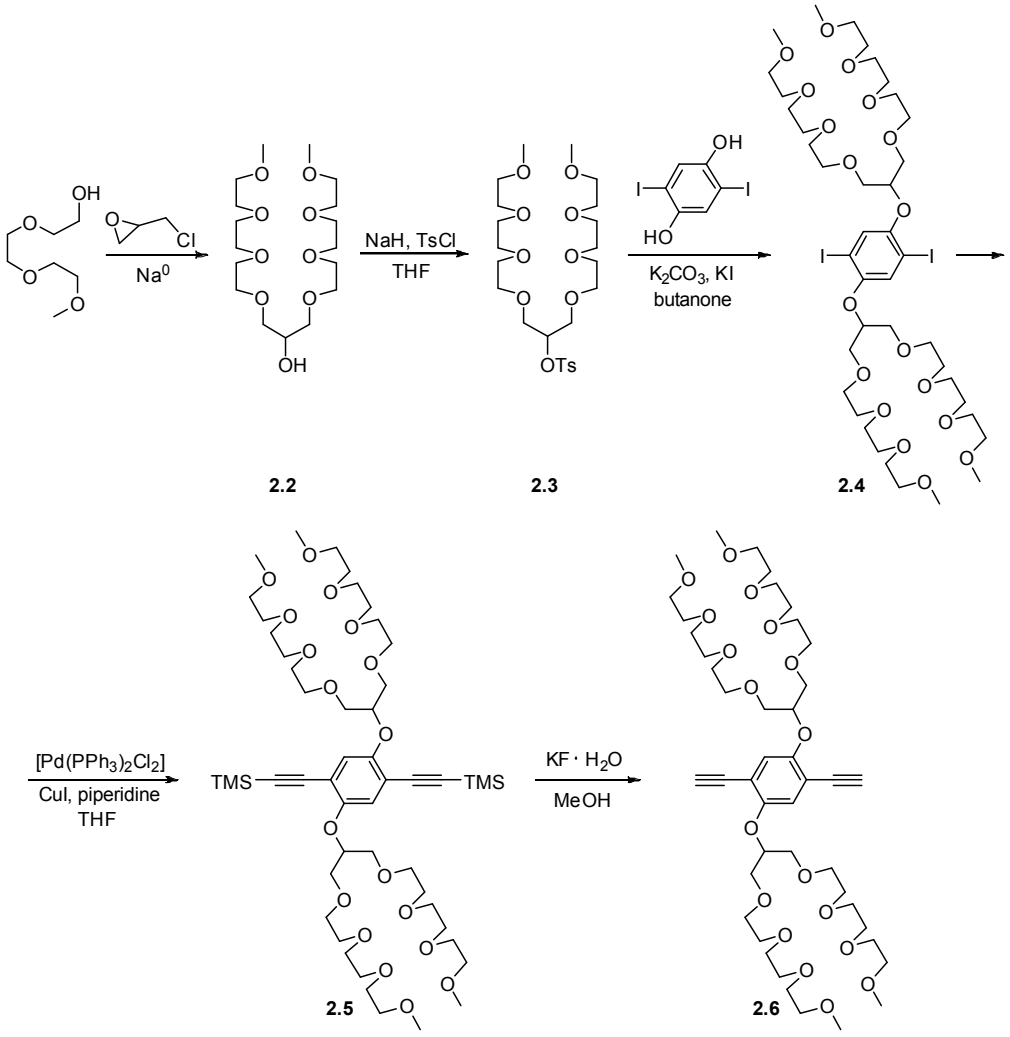

Figure 2.4 Synthesis of monomer **2.6**

The purpose of the swallowtail monomer in this instance is to provide a fourth polymer for the array. The swallowtail side chain helps to provide a polymer which interacts with analytes differently than the others in the array. The ease of swallowtail synthesis and its varied use in the Bunz group make it an obvious choice. Similar spectroscopic properties of polymer **2.7**, and sufficient solubility make it a fitting one.

The swallowtail side chain has found its way into other polymerization schemes as well. One example of the A_2 monomer **2.4** appearing elsewhere is the topic of the next section.

2.3 A Red-Emissive Water-Soluble PPE

2.3.1 Background

The vivid blue or green emission of many PPEs can be a problem for sensory applications in biological systems, which contain many fluorescent species that emit in the same region.[36] For biosensing, PPEs which emit at longer wavelengths would be advantageous, increasing the signal to noise ratio. Previous work in the Bunz group has demonstrated the tunability of PPEs when using conjugated side-chains.[21a] This is accomplished by using unsaturated substituents inspired by poly(*p*-phenylenevinylene)s (PPVs). This concept can be extended to the arena of biosensing by creating water-soluble polymers with the same type of unsaturated substituents. Copolymerization with the swallowtail monomer should help bring these materials into the aqueous phase. As part of the ongoing effort to tune the photophysical properties of water-soluble polymers, the cross-conjugated PPE shown in Figure 2.5 has been synthesized.

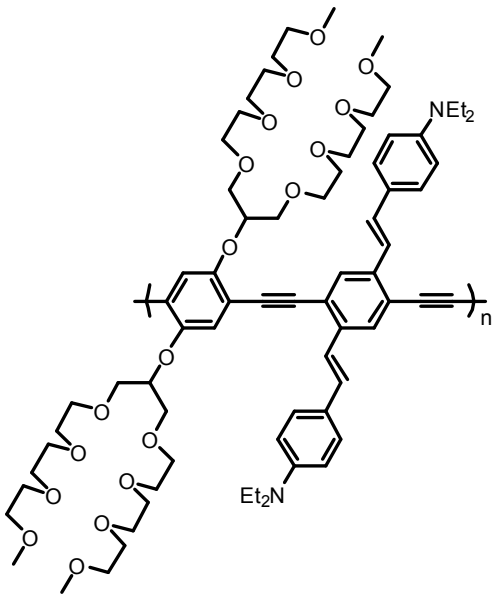

Figure 2.5 Water-soluble PPE-PPV hybrid

2.3.2 Discussion

Previous work in the Bunz group demonstrates the tunability of cruciforms[37] and PPEs[21a] containing conjugated side chains. Electron-donating substituents on the styryl axis were found to induce a bathochromic shift in the emission. The dimethylaminobenzene substituent used in this synthesis was chosen due to the effect it has shown on the emission of PPEs in these prior experiments. This amino functionality elicits a more bathochromic shift than either methyl benzoate or 1,3,5-trimethoxybenzene.[21a] These types of polymers also display some solvatochromicity, with lower energy emission maxima in more polar solvents.

Because of the expected solubility issues of a homopolymer containing this styryl side chain, a copolymer was made, using a monomer with swallowtail side chains. Incorporation of this monomer furnished a copolymer which exhibits solubility in a variety of organic solvents, as well as water.

2.4 Conclusions

A cationic copolymer containing swallowtail side chains was synthesized as part of a polymer array for glycan biosensing. The solubilizing properties of the swallowtail also serve to create a water-soluble, red-emissive PPE. This substituent will continue to find use in such systems due to its physical properties, and its ease of use.

2.5 Experimental

2.5.1 Synthesis of diethyl 2,2'-(1,4-phenylenebis(oxy))diacetate (2.1)

K_2CO_3 (33 g, 0.24 mol) and tetra-butylammonium bromide (4 g, 0.01 mol) were stirred in hot THF (150 mL) for 15 minutes. 2,5-Diiododihydroquinone (17.6 g, 0.0486 mol) was added to the mixture, followed by bromoethyl acetate (13.5 mL, 0.122 mol). After the reaction mixture was stirred at reflux for 2 d, an aqueous solution of $NaSO_3$ (100 mL) was used to quench the reaction. After extraction 3 times with CH_2Cl_2 (50

mL), the solvent was evaporated, and the product was recrystallized from EtOAc to yield a colorless solid (21.8 g, 0.0409 mol, 83%, m.p. 121-124°C). ^{1}H NMR (300 MHz, $CDCl_3$): δ 7.14 (s, 2H), 4.60 (s, 4H), 4.25 (q, 4H, J = 7 Hz), 1.29 (t, 6H, J = 7 Hz). ^{13}C NMR (75 MHz, $CDCl_3$): δ 167.93, 152.63, 123.51, 86.14, 67.21, 61.46, 14.10.

2.5.2 Synthesis of 2,5,8,11,15,18,21,24-octaoxapentacosan-13-ol (2.2)

Sodium metal (10. g, 0.43 mol) was stirred in tri(ethylene glycol) monomethyl ether (190 mL) in a dry flask at 100 °C for 2 h, until completely dissolved. The temperature was then reduced to 65 °C, and epichlorohydrin (32 mL, 0.41 mol) was added dropwise. The reaction was reheated to 100 °C and then allowed to stir for 24 h, after which time, NH_4Cl (22 g, 0.41 mol) was stirred in. The reaction mixture was then filtered through celite with $CHCl_2$, the solvent was evaporated, and the product was purified by vacuum distillation, yielding a colorless oil (79 g, 0.20 mol, 49%). ^{1}H NMR (300 MHz, $CDCl_3$): δ 3.76 (p, 1H, J = 5 Hz), 3.47 (m, 20H), 3.36 (m, 9H), 3.19 (s, 6H). ^{13}C NMR (75 MHz, $CDCl_3$): δ 72.66, 71.96, 70.78, 70.62, 70.59, 70.54, 70.53, 69.38, 59.02.

2.5.3 Synthesis of 2,5,8,11,15,18,21,24-octaoxapentacosan-13-yl 4-methylbenzenesulfonate (2.3)

NaH (1.4 g, 0.056 mol) was slowly added to a dry flask containing compound **2.2** (18.0 g, 0.0468 mol) and dry THF (50 mL). *para*-Toluenesulfonyl chloride (17.8 g, 0.0936 mol) was added and the reaction was stirred at room temperature overnight. Excess NaH was quenched by slowly adding H_2O (50 mL). The product was then extracted 3 times with $CHCl_3$ (50 mL), and the solvent was evaporated. After purification by silica gel chromatography (EtOAc), the product was recovered as a colorless oil (19.5 g, 0.036 mol, 77%). ^{1}H NMR (300 MHz, $CDCl_3$): δ 7.70 (d, 2H, J = 8 Hz), 7.22 (d, 2H, J = 8 Hz), 4.56 (p, 1H, J = 5 Hz), 3.51 (m, 16H), 3.42 (m, 12H), 3.26 (s,

6H), 2.33 (s, 3H). ^{13}C NMR (75 MHz, $CDCl_3$): δ 144.15, 133.61, 129.24, 127.60, 79.28, 71.51, 70.48, 70.18, 70.17, 70.10, 69.95, 69.24, 58.60, 21.25.

2.5.4 Synthesis of 13,13'-(2,5-diiodo-1,4-phenylene)bis(oxy) bis(2',5',8',11',15',18',21',24'-octaoxapentacosane) (2.4)

K_2CO_3 (15 g, 0.11 mol) and KI (0.4 g, 0.002 mol) were stirred into butanone (150 mL). 2,5-Diiododihydroquinone (7.84 g, 0.0217 mol) was then added, followed by compound **2.3** (24.52 g, 0.04552 mol). The reaction was stirred at reflux for 3 d, after which time the salts were filtered through celite with CH_2Cl_2. The solvent was evaporated, and silica gel chromatography (19:1 EtOAc:MeOH) afforded a pale yellow oil (13.4 g, 0.0122 mol, 56%). ^{1}H NMR (300 MHz, $CDCl_3$): δ 7.34 (s, 2H), 4.28 (p, 2H, J = 5 Hz), 3.62 (m, 8H), 3.55 (m, 40H), 3.44 (m, 8H), 3.26 (s, 12H). ^{13}C NMR (75 MHz, $CDCl_3$): δ 152.92, 125.59, 87.56, 80.44, 71.52, 70.79, 70.43, 70.26, 70.24, 70.19, 70.11, 58.65.

2.5.5 Synthesis of (2,5-bis(2,5,8,11,15,18,21,24-octaoxapentacosan-13-yloxy)-1,4-phenylene)bis(ethyne-2,1-diyl)bis(trimethylsilane) (2.5)

Compound **2.4** (4.6 g, 4.2 mmol) was dissolved in dry THF (5 mL). Piperidine (5 mL) was added, and the mixture was stirred under N_2(g) for 10 min. $Pd(PPh_3)_3Cl_2$ (29 mg, 0.042 mmol) and CuI (8 mg, 0.04 mmol) were subsequently added under N_2(g). The reaction mixture was sealed, and trimethylsilyl acetylene (2.42 mL, 16.8 mmol) was added via syringe. After stirring at room temperature for 2 d, the solids were filtered, solvent was evaporated, and the product was purified by silica gel chromatography (19:1 EtOAc:MeOH), yielding a light yellow oil (3.57 g, 3.44 mmol, 82%). ^{1}H NMR (300 MHz, $CDCl_3$): δ 6.98 (s, 2H), 4.33 (p, 2H, J = 5 Hz), 3.64 (m, 8H), 3.55 (m, 40H), 3.46 (m, 8H), 3.27 (s, 12H), 0.14 (s, 18H). ^{13}C NMR (75 MHz, $CDCl_3$): δ 153.62, 121.03,

115.53, 100.78, 99.67, 79.55, 71.60, 70.87, 70.31, 70.30, 70.26, 70.20, 70.19, 58.70, -0.32.

2.5.6 Synthesis of 13,13'-(2,5-diethynyl-1,4-phenylene)bis(oxy) bis(2',5',8',11',15',18',21',24'-octaoxapentacosane) (2.6)

Compound **2.5** (2.96 g, 2.85 mmol) and $KF{\cdot}H_2O$ (0.87 g, 11 mmol) were stirred in MeOH (25 mL) overnight. H_2O was added, and the solution was then extracted 3 times with $CHCl_3$ (25 mL). Solvent was evaporated, and the product was purified by silica gel chromatography (19:1 EtOAc:MeOH). A light yellow oil was recovered (1.82 g, 2.04 mmol, 71%). ^{1}H NMR (300 MHz, $CDCl_3$): δ 7.06 (s, 2H), 4.33 (p, 2H, J = 5 Hz), 3.63 (m, 8H), 3.55 (m, 40H), 3.45 (m, 8H), 3.26 (s, 12H), 3.25 (s, 2H). ^{13}C NMR (75 MHz, $CDCl_3$): δ 154.30, 121.66, 115.18, 82.97, 80.17, 79.86, 72.05, 71.30, 70.77, 70.76, 70.75, 70.70, 70.63, 59.14.

2.5.7 Synthesis of PPE 2.7

Monomer **2.6** (0.300 g, 0.336 mmol), monomer **2.1** (0.180 g, 0.336 mmol), and triethylamine (1 mL) were stirred into THF (1 mL) and toluene (1 mL). After degassing, $Pd(PPh_3)_2Cl_2$ (2.4 mg, 0.0034 mmol) and CuI (1.3 mg, 0.0067 mmol) were added under N_2(g). After stirring at 45 °C for 2 d, H_2O was added, and the solution was extracted 3 times with $CHCl_3$ (25 mL). After precipitation into hexane, the product was filtered and recovered as a yellow solid (247 mg, 0.211 mmol, 63%). GPC (THF, polystyrene standard) M_w 13041; M_n 10340. ^{1}H NMR (300 MHz, $CDCl_3$): δ 7.22 (s, 2H), 7.03 (s, 2H), 4.77 (m, 4H), 4.61 (m, 2H), 4.28 (m, 4H), 3.79 (m, 8H), 3.67 (m, 8H), 3.62 (m, 32H), 3.51 (m, 8H), 3.35 (s, 12H), 1.31 (t, 6H, J = 7 Hz). ^{13}C NMR (75 MHz, $CDCl_3$): δ 168.68, 153.43, 122.17, 120.65, 118.86, 115.77, 114.89, 92.44, 90.63, 80.75, 71.84, 71.14, 71.05, 70.52, 70.51, 70.47, 70.41, 67.11, 61.23, 58.98, 14.21.

2.5.8 Synthesis of PPE 2.8

Polymer **2.7** (247 mg) and *N*,*N*-dimethylethylenediamine (0.1 mL) were stirred in MeOH (50 mL) at 50 ºC for 24 h. After removal of the solvent, the residue was washed thoroughly with hexane. After being dried under vacuum, polymer **2.8** was obtained as a yellow powder (256 mg, 0.204 mmol, 97%). ^{1}H NMR (300 MHz, $CDCl_3$): δ 7.24 (s, 2H), 6.94 (s, 2H), 4.52 (s, 4H), 4.39 (m, 2H), 3.74 (m, 56H), 3.31 (m, 4H), 3.26 (s, 12H), 2.42 (m, 4H), 2.17 (s, 12H).

2.5.9 Synthesis of PPE 2b

2.8 (256 mg) was dissolved in CH_2Cl_2 (50 mL) and iodomethane (0.5 mL). The reaction mixture was stirred at room temperature overnight. Water was then added, and the solution was washed 3 times with hexane (25 mL). After dialysis for 3 d, the polymer solution was lyophilized to yield a yellow solid (246 mg, 0.191 mmol, 94%). ^{1}H NMR (300 MHz, D_2O): δ 7.24 (s, 2H), 6.94 (s, 2H), 4.60 (s, 4H), 4.39 (m, 2H), 3.76 (m, 56H), 3.36 (m, 4H), 3.17 (s, 12H), 2.51 (m, 4H), 2.26 (s, 18H).

CHAPTER 3

PLASMONIC FIELD ENHANCEMENT OF AN AMPIPHILIC FLUORESCENT POLYMER

3.1 Introduction

One distinct characteristic of metallic nanoparticles is their surface plasmon resonance (SPR). This phenomenon has found widespread application in biosensing,[38] as well as surface enhanced Raman spectroscopy.[39] When irradiated with light of the proper wavelength, the surface plasmon resonance induces strong electromagnetic fields in the vicinity of the nanoparticle.[40] This leads to an enhancement of the electronic properties of nearby systems, such as conjugated polymers.[41] Previous work by Mahmoud, *et al.* explores the effect of metallic nanoparticles on a poly(*p*-phenyleneethynylene) (PPE).[42] Specifically, PPE **3** (provided by the Bunz lab) was deposited as a monolayer on silver nanocubes.

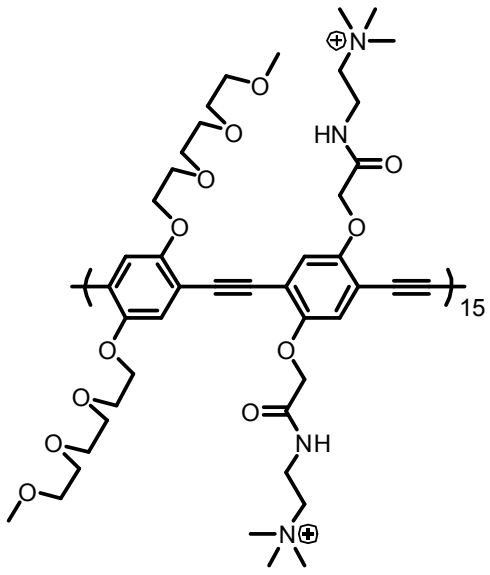

3

Figure 3.1 PPE **3**

This polymer was deposited on the nanocubes as a monolayer using the Langmuir-Blodgett technique with water as a base. This involves depositing the polymer as a solution in chloroform, and allowing the solvent to evaporate. A polymer that exhibits solubility in both chloroform and water is needed, and the ampiphilic PPE **3** works quite well.

Upon irradiation, the SPR generated by the nanoparticles amplifies the electronic properties of the polymer. The rate of absorption was enhanced, leading to increased fluorescent intensity. This amplified fluorescence is seen to increase as a function of nanoparticle surface density, up to a certain point, where the fluorescent intensity is seen to decrease.

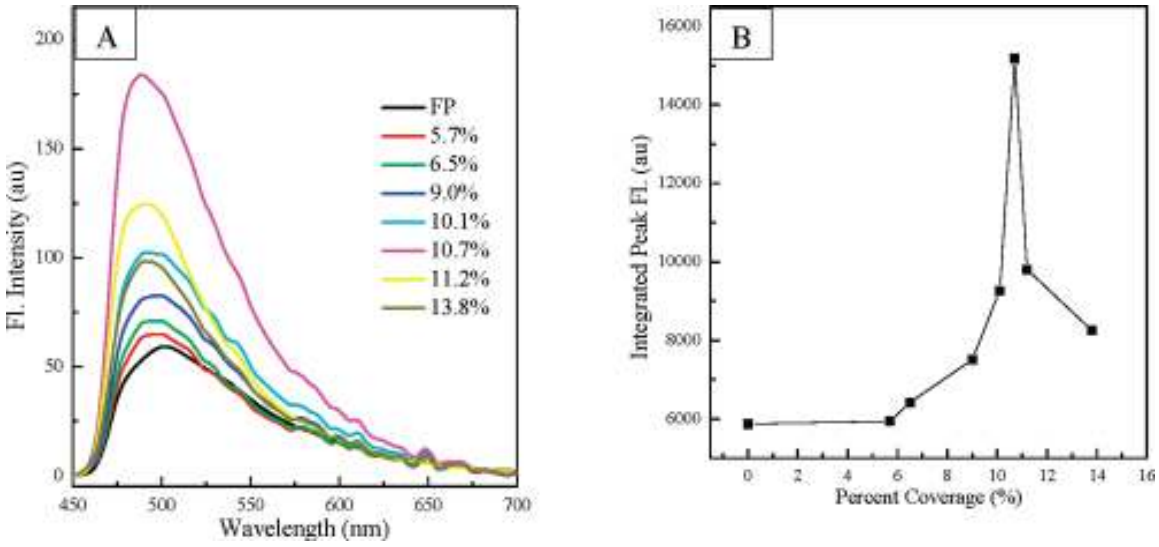

Figure 3.2 (A) Fluoresence spectra of PPE monolayer deposited on silver nanocubes as a function of nanocube surface density. (B) Integrated fluorescent intensity as a function of nanocube surface density.[42] (Courtesy of the El-Sayed group)

Mahmoud, *et al*., postulate that at this threshold surface density (around 11.2%), there are so many absorbed photons that exciton-exciton annihilation becomes a faster process than fluorescence.[42] In order to investigate the effect of conjugation length on these competing processes, we set out to synthesize polymer **3** with different molecular weights.

3.2 Discussion

In order to deposit PPE **3** as a Langmuir-Blodgett film onto water, it must display some solubility in water, as well as organic solvents. The experiments also require that the polymer possess some spectral overlap with the silver nanocubes. Tri(ethylene glycol) side chains are used in this polymer to help provide an ampiphilic nature. The spectroscopic requirements are also fulfilled, with an absorption maximum very near the nanocube absorption maximum. Polymer **3** was synthesized in three separate batches; the same procedure was used for each polymerization (Figure 3.3). Polymerization of monomers **3.1** and **3.5** gave polymer **3.6**. Post-functionalization of PPE **3.6** with *N*,*N*-dimethylethylenediamine yielded PPE **3.7**, and methylation of **3.7** led to PPE **3**.

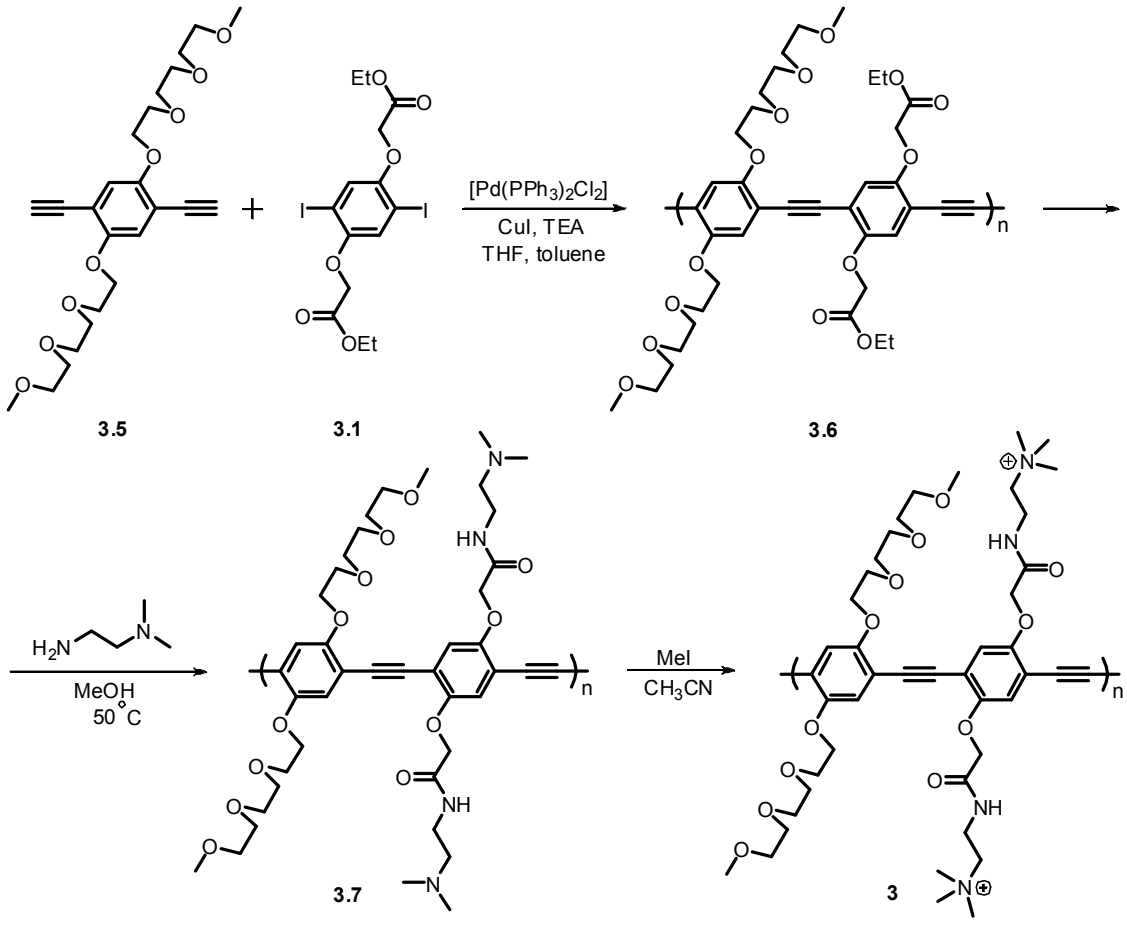

Figure 3.3 Synthetic scheme for PPE **3**

Photophysical properties of polymers **3.6** and **3.7** were very similar for each separate polymer. Absorption and emission spectra are shown in Figure 3.5. Three samples of **3** were synthesized, and gel permeation chromatography was used to determine number average molecular weights of 15350, 18058, and 26412. Absorption and emission spectra of PPEs **3** are shown in Figure 3.6.

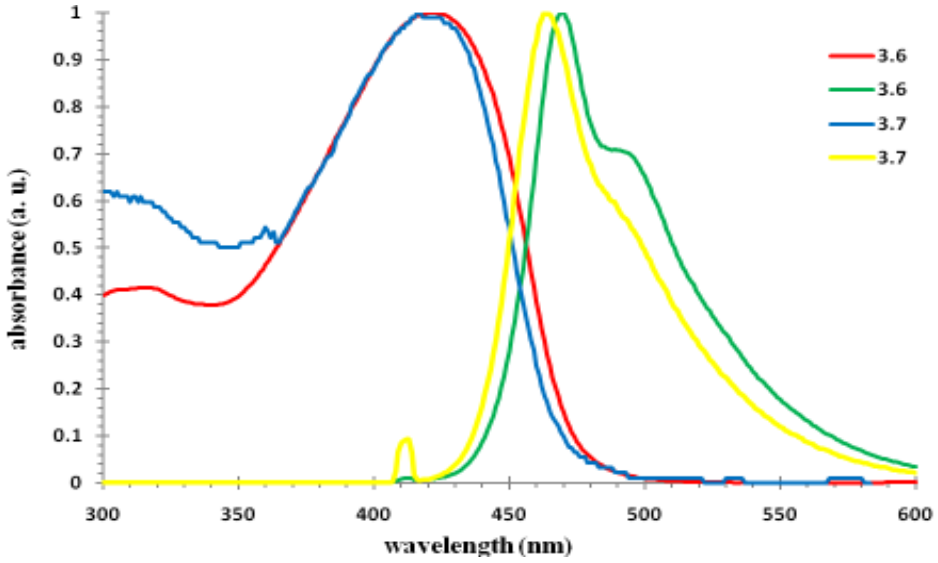

Figure 3.4 Normalized absorption (red and blue) and emission (green and yellow) spectra of PPEs **3.6** and **3.7** in $CHCl_3$

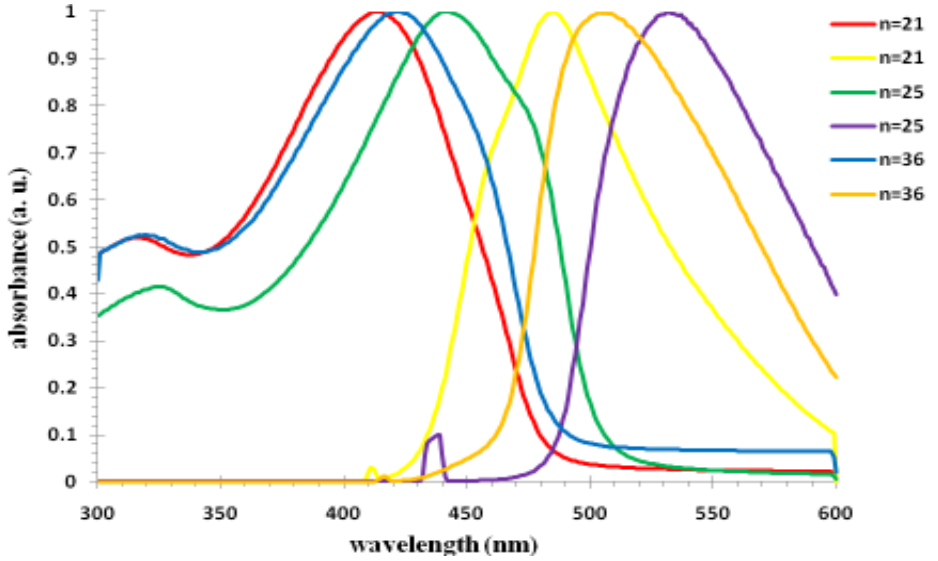

Figure 3.5 Normalized absorption (red, blue, and green) and emission (orange, yellow, and purple) spectra of PPEs **3** in H_2O

Monomer **3.1** was synthesized through alkylation of 2,5-diiododihydroquinone with bromoethylacetate. Monomer **3.5** was reached as shown in Figure 3.4. Tri(ethylene glycol) monomethyl ether was tosylated, and then added to 2,5-diiododihydroquinone to give the A_2 monomer **3.3**. Trimethylsilyl acetylene was then added via Sonogashira coupling, and subsequent deprotection with potassium fluoride hydrate yielded the B_2 monomer **3.5**.

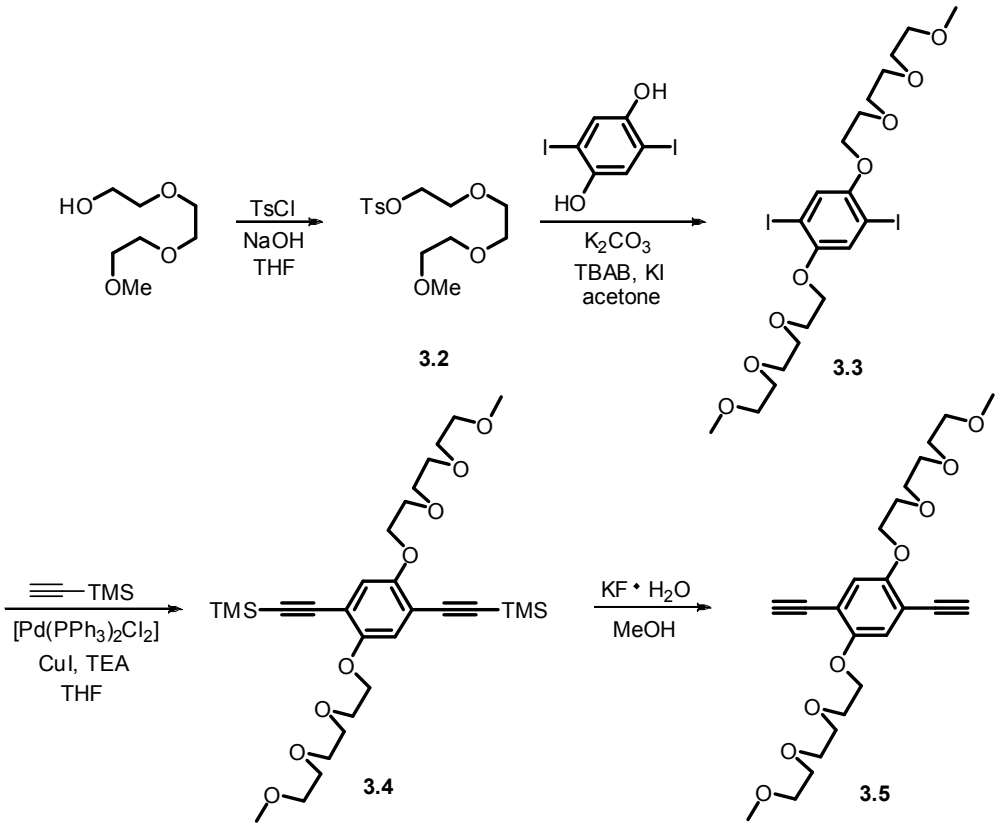

Figure 3.6 Synthetic scheme for monomer **3.5**

3.3 Conclusions

An ampiphilic ethylene-glycol containing polymer has been synthesized in different molecular weights. After deposition onto silver nanocubes, these polymers will be used for an exciton-exciton annihilation study. We expect to find that increasing conjugation length will increase the rate of annihilation, due to an increase in intrachain

exciton collisions. The results will further understanding of the role that surface plasmon resonance plays in these competing one- and two-photon processes, as well as its effect on nearby conjugated polymers.

3.4 Experimental

3.4.1 Synthesis of diethyl 2,2'-(1,4-phenylenebis(oxy))diacetate (3.1)

K_2CO_3 (33 g, 0.24 mol) and tetra-butylammonium bromide (4 g, 0.01 mol) were stirred in hot THF (150 mL) for 15 minutes. 2,5-Diiododihydroquinone (17.6 g, 0.0486 mol) was added to the mixture, followed by bromoethyl acetate (13.5 mL, 0.122 mol). After the reaction mixture was stirred at reflux for 2 d, an aqueous solution of $NaSO_3$ (100 mL) was used to quench the reaction. After extraction 3 times with CH_2Cl_2 (100 mL), the solvent was evaporated, and the product was recrystallized from EtOAc to yield a colorless solid (21.8 g, 0.0409 mol, 83%, m.p. 121-124 °C). ^{1}H NMR (300 MHz, $CDCl_3$): δ 7.14 (s, 2H), 4.60 (s, 4H), 4.25 (q, 4H, J = 7 Hz), 1.29 (t, 6H, J = 7 Hz). ^{13}C NMR (75 MHz, $CDCl_3$): δ 167.93, 152.63, 123.51, 86.14, 67.21, 61.46, 14.10.

3.4.2 Synthesis of 2-(2-(2-methoxyethoxy)ethoxy)ethyl 4-methylbenzenesulfonate (3.2)

Tri(ethylene glycol) monomethyl ether (50.0 g, 0.304 mol) and *para*-toluenesulfonyl chloride (116 g, 0.609 mol) were dissolved in THF (200 mL). The reaction mixture was then cooled to 0 °C, and NaOH (36.5 g, 0.913 mol) was added dropwise as an aqueous solution. After stirring overnight, the solution was extracted 3 times with $CHCl_3$ (100 mL). The solvent was evaporated, and purification by silica gel chromatography (9:1 hexane:EtOAc for excess TsCl, followed by 1:1 hexane:EtOAc), yielded the product as a colorless oil (71.3 g, 0.224 mol, 74%). ^{1}H NMR (300 MHz, $CDCl_3$): δ 7.66 (d, 2H, J = 8 Hz), 7.23 (d, 2H, J = 8 Hz), 4.03 (t, 2H, J = 5 Hz), 3.55 (t, 2H, J = 5 Hz), 3.46 (m, 6H), 3.39 (m, 2H), 3.23 (s, 3H), 2.32 (s, 3H). ^{13}C NMR (75

MHz, $CDCl_3$): δ 144.42, 132.52, 129.44, 127.49, 71.43, 70.22, 70.06, 70.05, 68.94, 68.17, 58.51, 21.17.

3.4.3 Synthesis of 1,4-diiodo-2,5-bis(2-(2-(2-methoxyethoxy)ethoxy)ethoxy)benzene (3.3)

K_2CO_3 (29.6g, 0.214 mol) and tetra-butylammonium bromide (3 g, 0.01 mol) were stirred into acetone (150 mL) for ten minutes. 2,5-Diiododihydroquinone (12.9 g, 0.0356 mol) and KI (0.6 g, 0.004 mol) were then added to the mixture, followed by compound **3.2** (25.0 g, 0.0785 mol). The reaction was stirred at reflux for 3 d. The solids were then filtered through celite with CH_2Cl_2, the solvent was evaporated, and the product was purified by silica gel chromatography (3:1 hexane:EtOAc for starting material, EtOAc for product) to give a pale yellow oil (18.4 g, 0.0282 mol, 79%). ^{1}H NMR (300 MHz, $CDCl_3$): δ 7.18 (s, 2H), 4.05 (t, 4H, J =5 Hz), 3.82 (t, 4H, J = 5 Hz), 3.74 (m, 4H), 3.62 (m, 8H), 3.50 (m, 4H), 3.32 (s, 6H). ^{13}C NMR (75 MHz, $CDCl_3$): δ 153.02, 123.37, 86.38, 71.90, 71.10, 70.71, 70.54, 70.23, 69.56, 59.03.

3.4.4 Synthesis of (2,5-bis(2-(2-(2-methoxyethoxy)ethoxy)ethoxy)-1,4-phenylene)bis(ethyne-2,1-diyl)bis(trimethylsilane) (3.4)

Compound **3.3** (11.3 g, 17.3 mmol) and triethylamine (1 mL) were stirred in THF (20 mL) under N_2(g) for 15 min. $Pd(PPh_3)_2Cl_2$ (0.12 g, 0.17 mmol) and CuI (0.065 g, 0.34 mmol) were added under N_2(g). The reaction was sealed, and trimethylsilyl acetylene (12.3 mL, 86.4 mmol) was added via syringe. The reaction was stirred for 2 d, and then extracted 3 times with H_2O and $CHCl_3$ (50 mL). The product was purified by silica gel chromatography (5:1 hexane:EtOAc), yielding a light tan powder (7.41 g, 12.4 mmol, 72%). ^{1}H NMR (300 MHz, $CDCl_3$): δ 6.90 (s, 2H), 4.11 (t, 4H, J = 5 Hz), 3.86 (t, 4H, J = 5 Hz), 3.76 (m, 4H), 3.65 (m, 8H), 3.55 (m, 4H), 3.36 (s, 6H), 0.23 (s, 18H). ^{13}C

NMR (75 MHz, $CDCl_3$): δ 153.81, 117.67, 114.09, 100.78, 100.32, 71.88, 71.11, 70.74, 70.50, 69.63, 69.46, 58.99, -0.09.

3.4.5 Synthesis of 1,4-bis(2-(2-(2-methoxyethoxy)ethoxy)ethoxy)-2,5-di(prop-1-ynyl)benzene (3.5)

Compound **3.4** (2.6 g, 4.4 mmol) and potassium fluoride hydrate (1.7 g, 22 mmol) were dissolved in MeOH (25 mL) and stirred overnight. The reaction was then extracted 3 times with H_2O and $CHCl_3$ (50 mL), the solvent was evaporated, and the product was purified with a silica gel plug (hexane for TMS, CH_2Cl_2 for the product). A light tan solid was recovered (1.5 g, 3.3 mmol, 76%, m.p. 50-51 °C). ^{1}H NMR (300 MHz, $CDCl_3$): δ 6.99 (s, 2H), 4.14 (t, 4H, J = 5 Hz), 3.86 (t, 4H, J = 5 Hz), 3.77 (m, 4H), 3.66 (m, 8H), 3.54 (m, 4H), 3.37 (s, 6H), 3.32 (s, 2H). ^{13}C NMR (75 MHz, $CDCl_3$): δ 154.01, 118.22, 113.51, 82.79, 79.53, 71.92, 71.03, 70.68, 70.54, 69.56, 69.45, 59.02.

3.4.6 Synthesis of PPE 3.6

Monomers **3.1** (564 mg, 1.04 mmol) and **3.5** (500. mg, 1.11 mmol) were added to a solution of toluene (5 mL), THF (1 mL), and triethylamine (1 mL). After degassing via the freeze/pump/thaw method, $Pd(PPh_3)_2Cl_2$ (74 mg, 0.010 mmol) and CuI (40. mg, 0.021 mmol) were added under N_2(g). After stirring at room temperature for 3 d, the reaction mixture was then precipitated into hexane, and the polymer was filtered, dried under vacuum, and recovered as an orange powder (660. mg, 0.895 mmol, 91%). GPC (THF, polystyrene standard) Polymer 1: M_w 37786; M_n 15350. Polymer 2: M_w 21484; M_n 18058. Polymer 3: M_w 43728; M_n 26412. ^{1}H NMR (300 MHz, $CDCl_3$): δ 7.10 (s, 2H), 7.02 (s, 2H), 4.75 (s, 4H), 4.24 (m, 8H), 3.91 (m, 4H), 3.76 (m, 4H), 3.61 (m, 8H), 3.50 (m, 4H), 3.33 (s, 6H), 1.29 (t, 6H, J = 7 Hz). ^{13}C NMR (75 MHz, $CDCl_3$): δ 168.64, 153.53, 126.15, 118.90, 117.76, 114.95, 114.35, 92.56, 90.80, 71.86, 70.94, 70.66, 70.48, 69.60, 69.40, 67.23, 61.30, 58.97, 14.21.

3.4.7 Synthesis of PPE 3.7

Polymer **3.6** (660 mg) and *N,N*-dimethylethylenediamine (1 mL) were stirred in THF (10 mL) at 50 °C overnight. The reaction mixture was then extracted 3 times with H_2O and $CHCl_3$ (25 mL), and the solvent was evaporated to give the product as an orange powder (460 mg, 0.57 mmol, 63%). ^{1}H NMR (300 MHz, $CDCl_3$): δ 7.12 (s, 2H), 7.07(s, 2H), 4.63 (s, 4H), 4.24 (m, 4H), 3.88 (m, 4H), 3.72 (m, 4H), 3.61 (m, 8H), 3.48 (m, 8H), 3.34 (s, 6H), 2.17 (s, 12H).

3.4.8 Synthesis of PPE 3

Polymer **3.7** (460 mg, 0.57 mmol) and iodomethane (0.5 mL, 8 mmol) were stirred in CH_3CN overnight. H_2O was added to the solution, and it was then washed 3 times with hexane (25 mL). After dialysis of the water-soluble polymer for 5 d, the polymer solution was lyophilized to give a yellow solid (450 mg, 0.54 mmol, 95%). ^{1}H NMR (300 MHz, D_2O): δ 7.18 (s, 2H), 7.07 (s, 2H), 4.38 (m, 4H), 4.01 (m, 4H), 3.84 (m, 4H), 3.66 (m, 8H), 3.55 (m, 16H), 3.32 (s, 6H), 3.20 (s, 18H).

APPENDIX A

SYNTHESIS OF 2,5-DIIODODIHYDROQUINONE

2,5-diiodo(*p*-dimethoxybenzene)

Iodine (69 g, 0.27 mol), *p*-dimethoxybenzene (50. g, 0.36 mol), KIO_4 (83 g, 0.36 mol), and sulfuric acid (5 mL) were dissolved in acetic acid (750 mL). The reaction was stirred overnight under a condenser at 90 °C. The reaction was then quenched with an aqueous solution of $NaSO_3$ (500 mL) until the purple color subsided and the solution turned a yellow color. The solid product was then filtered off, washed with H_2O, and dried, yielding a light beige powder (106 g, 0.273 mol, 76%, m.p. 170-173 °C). ^{1}H NMR (300 MHz, $CDCl_3$): δ 7.18 (s, 2H), 3.82 (s, 6H). ^{13}C NMR (75 MHz, $CDCl_3$): δ 153.19, 121.47, 85.39, 57.11.

2,5-diiododihydroquinone

2,5-Diiodo(*p*-dimethoxybenzene) (20.0 g, 0.0513 mol) was dissolved in CH_2Cl_2 (500 mL). The solution was cooled to 0°C, and BBr_3 (9.7 mL, 0.205 mol) was added under N_2(g). After the reaction was stirred at room temperature overnight, it was slowly quenched with H_2O. The solid product crashed out, and was filtered and dried, yielding a fluffy off-white powder (16.2 g, 0.0447 mol, 87%, m.p. 198-201 °C). ^{1}H NMR (300 MHz, DMSO): δ 9.80 (s, 2H), 7.12 (s, 2H). ^{13}C NMR (75 MHz, DMSO): δ 150.36, 123.54, 84.31.

APPENDIX B

NMR SPECTRA

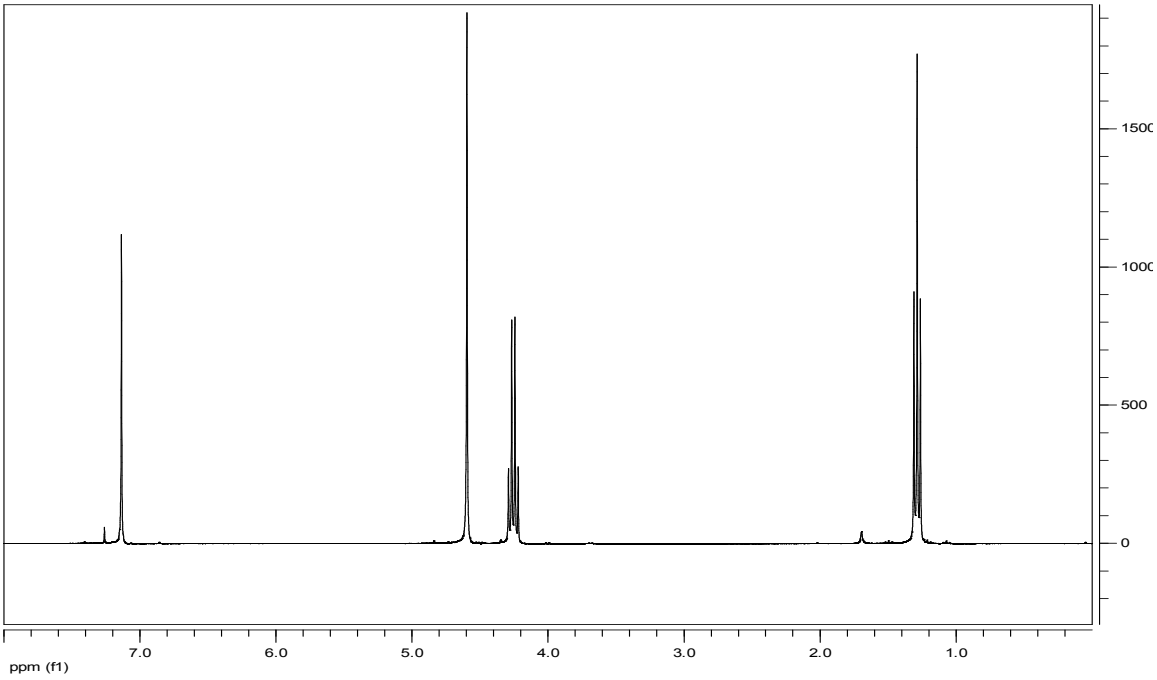

Figure B.1 ^{1}H NMR spectrum of **2.1** and **3.1** in $CDCl_3$

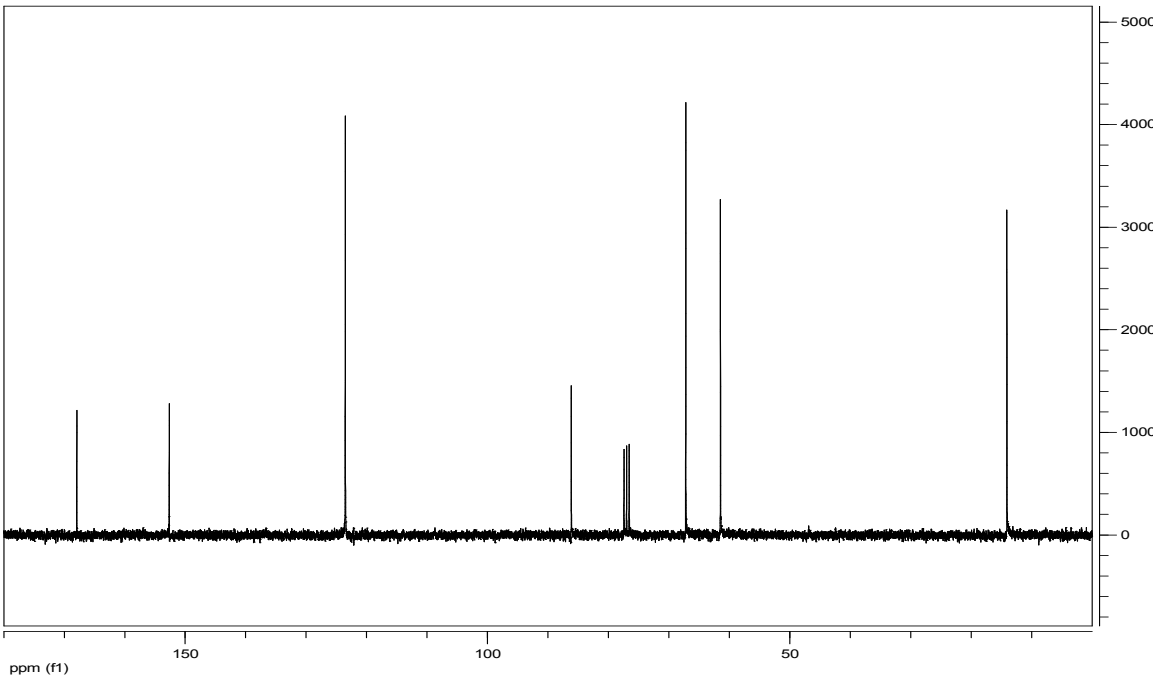

Figure B.2 ^{13}C NMR spectrum of **2.1** and **3.1** in $CDCl_3$

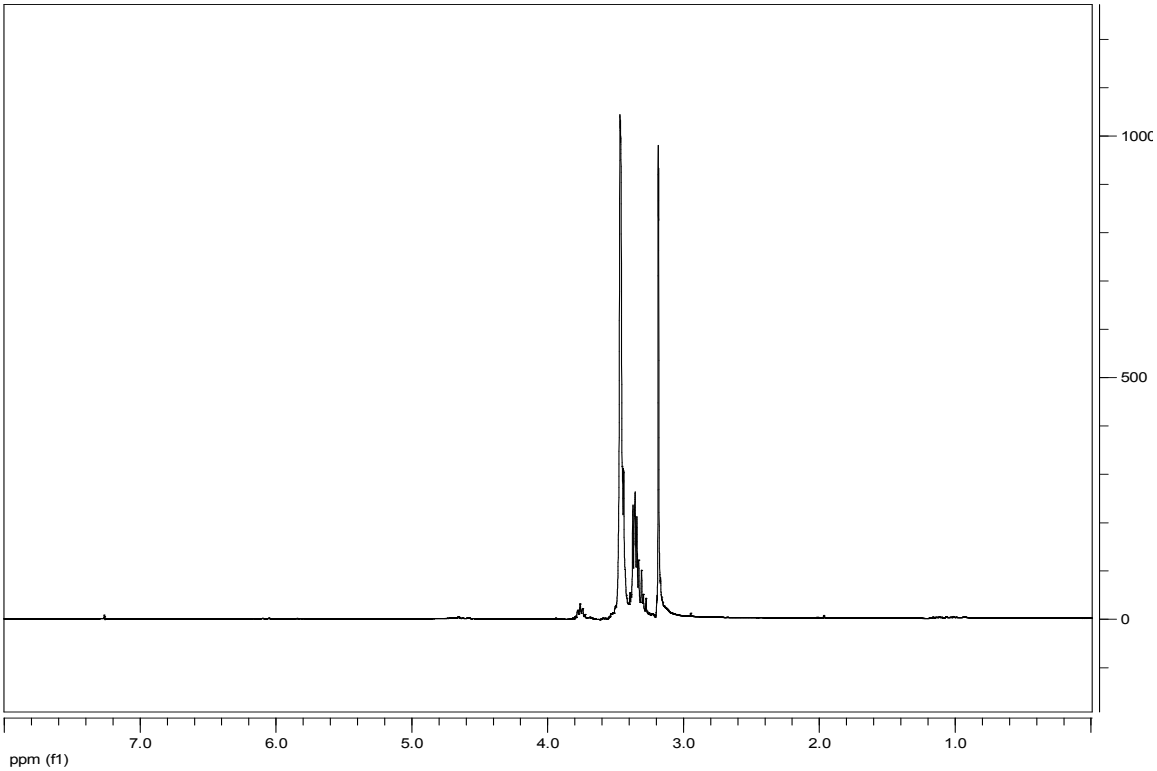

Figure B.3 ^{1}H NMR spectrum of **2.2** in $CDCl_3$

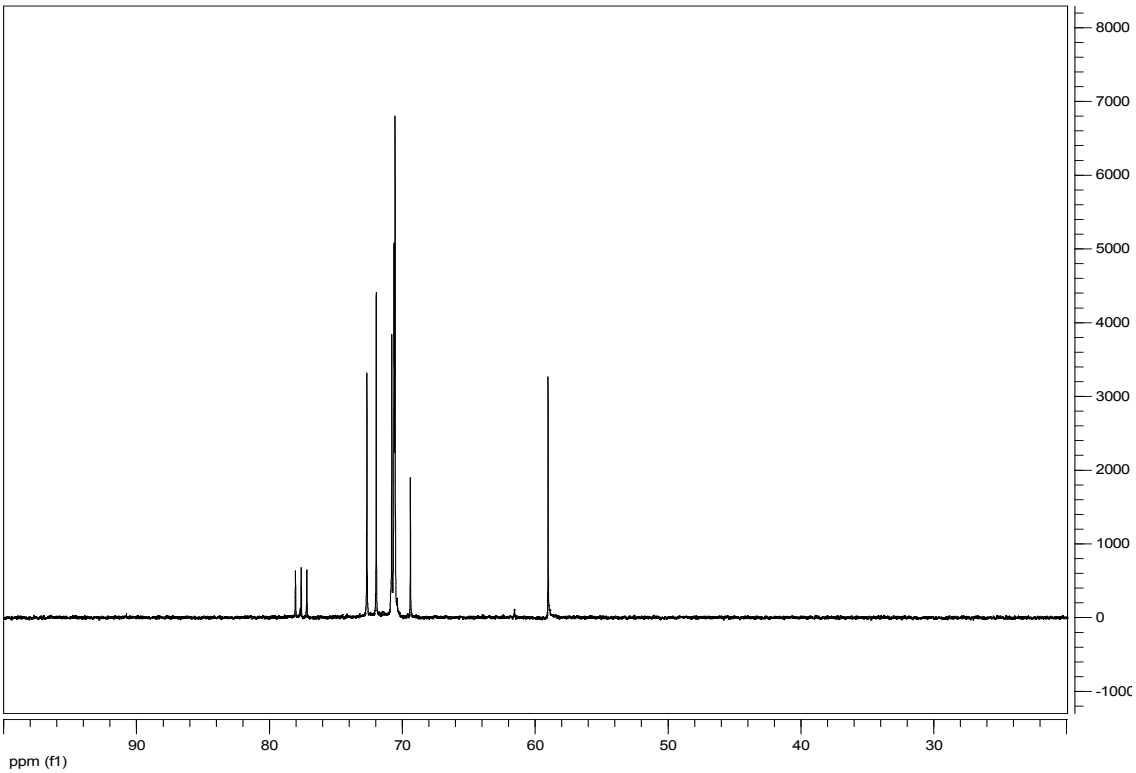

Figure B.4 ^{13}C NMR spectrum of **2.2** in $CDCl_3$

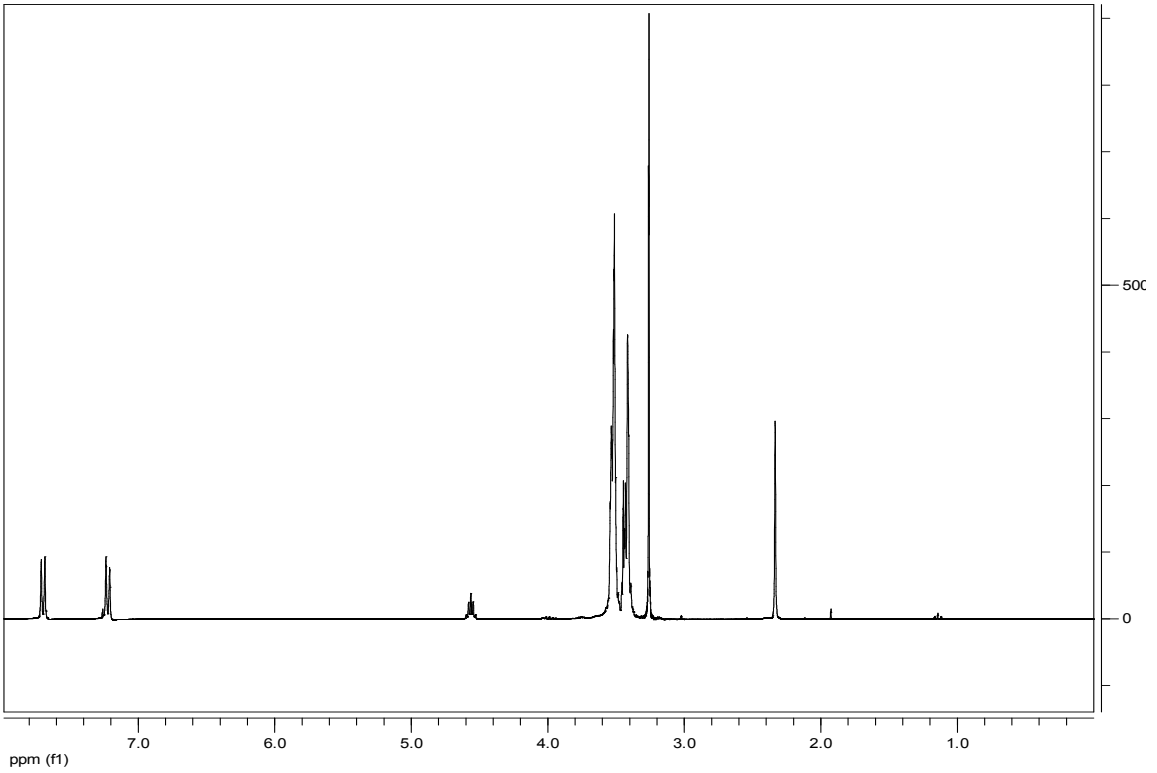

Figure B.5 ^{1}H NMR spectrum of **2.3** in $CDCl_3$

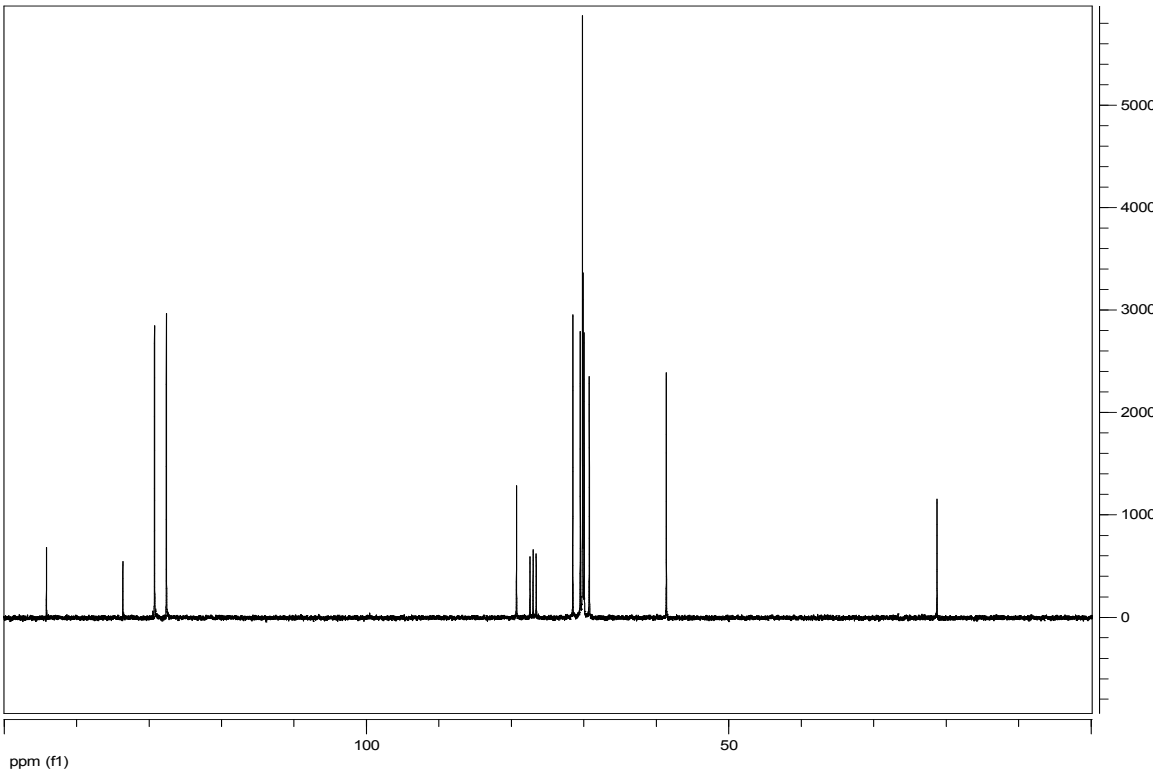

Figure B.6 ^{13}C NMR spectrum of **2.3** in $CDCl_3$

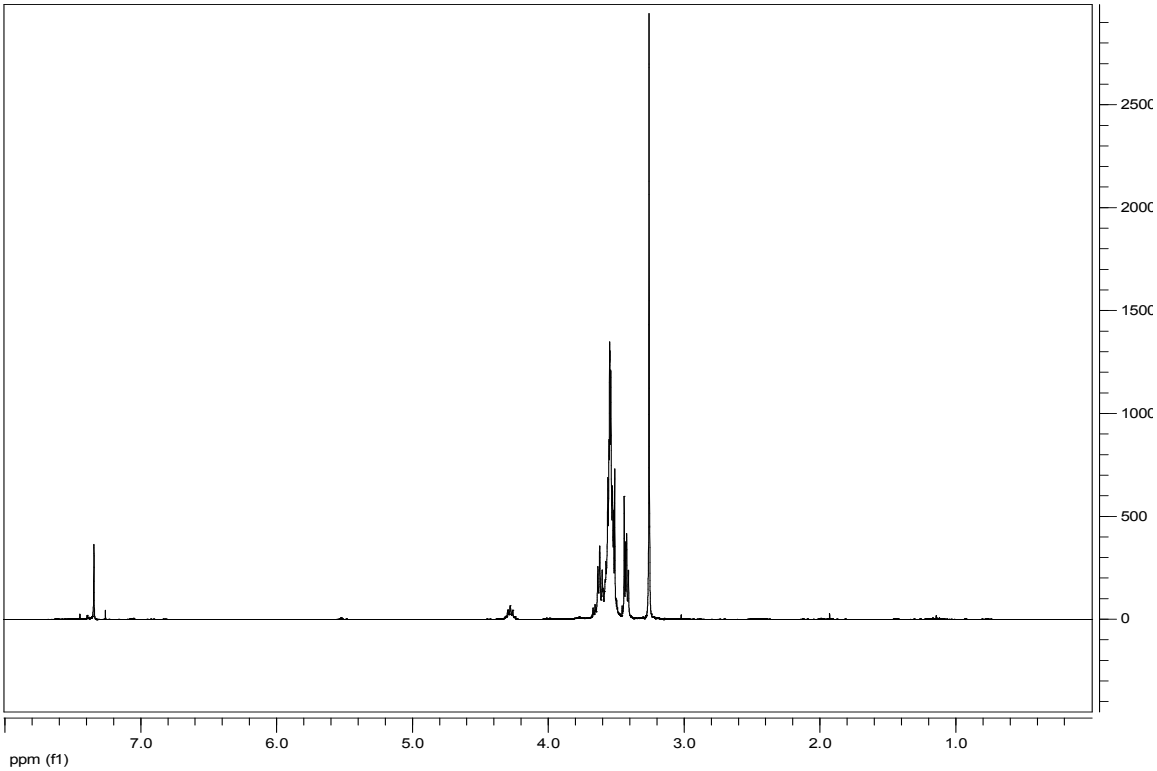

Figure B.7 ^{1}H NMR spectrum of **2.4** in $CDCl_3$

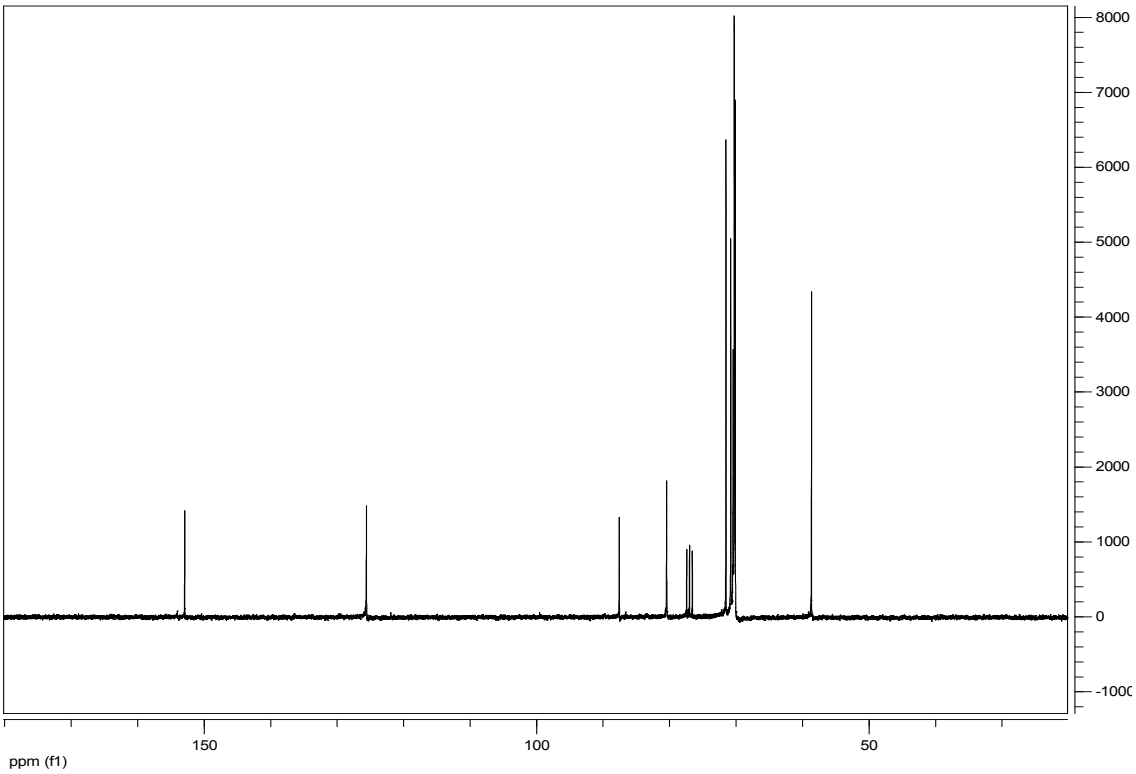

Figure B.8 ^{13}C NMR spectrum of **2.4** in $CDCl_3$

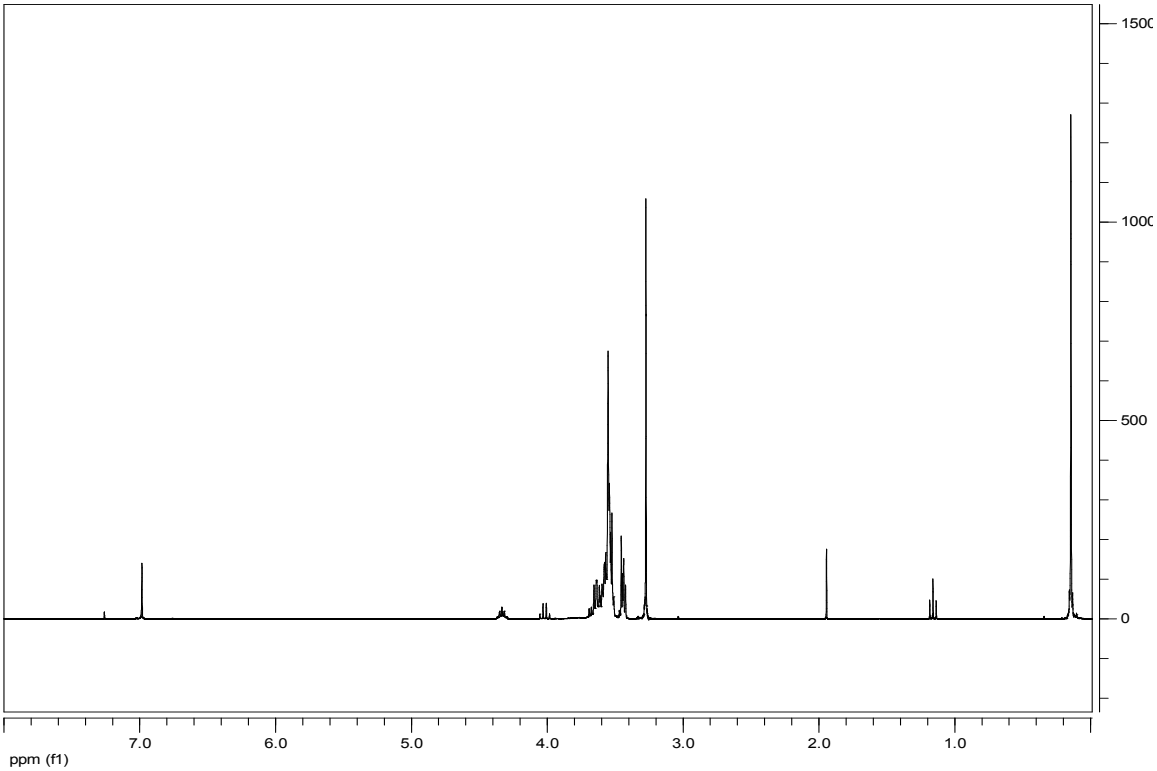

Figure B.9 ^{1}H NMR spectrum of **2.5** in $CDCl_3$

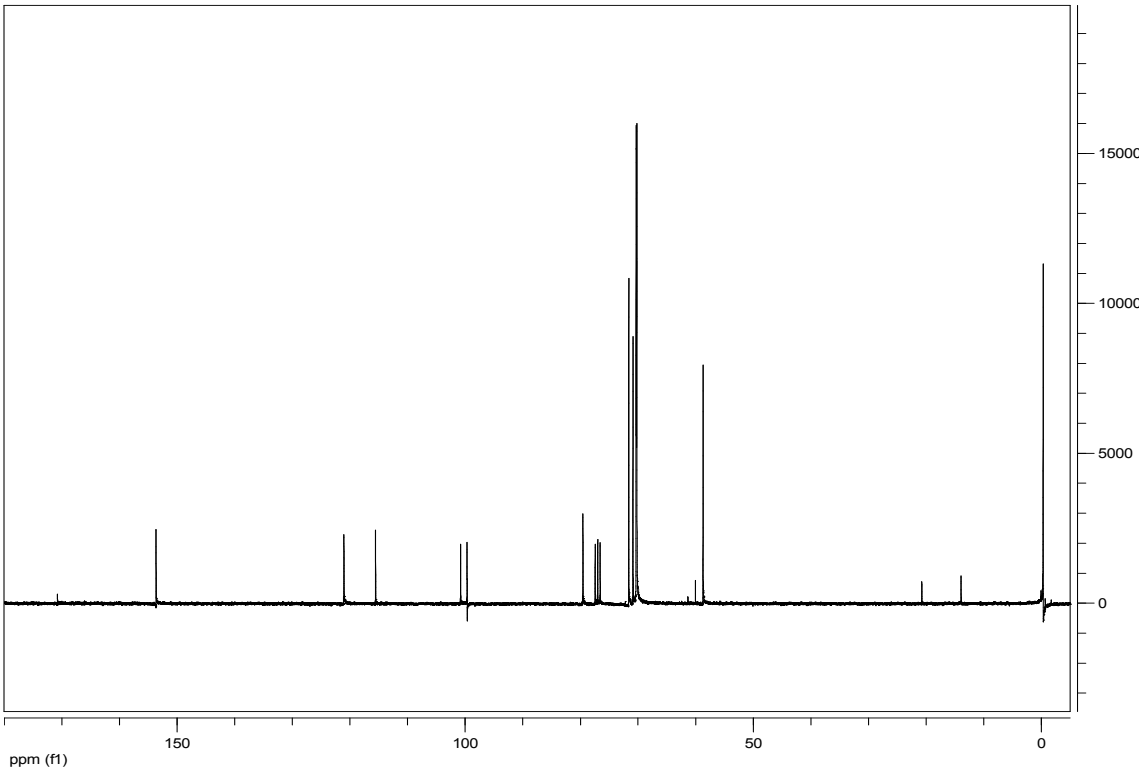

Figure B.10 ^{13}C NMR spectrum of **2.5** in $CDCl_3$

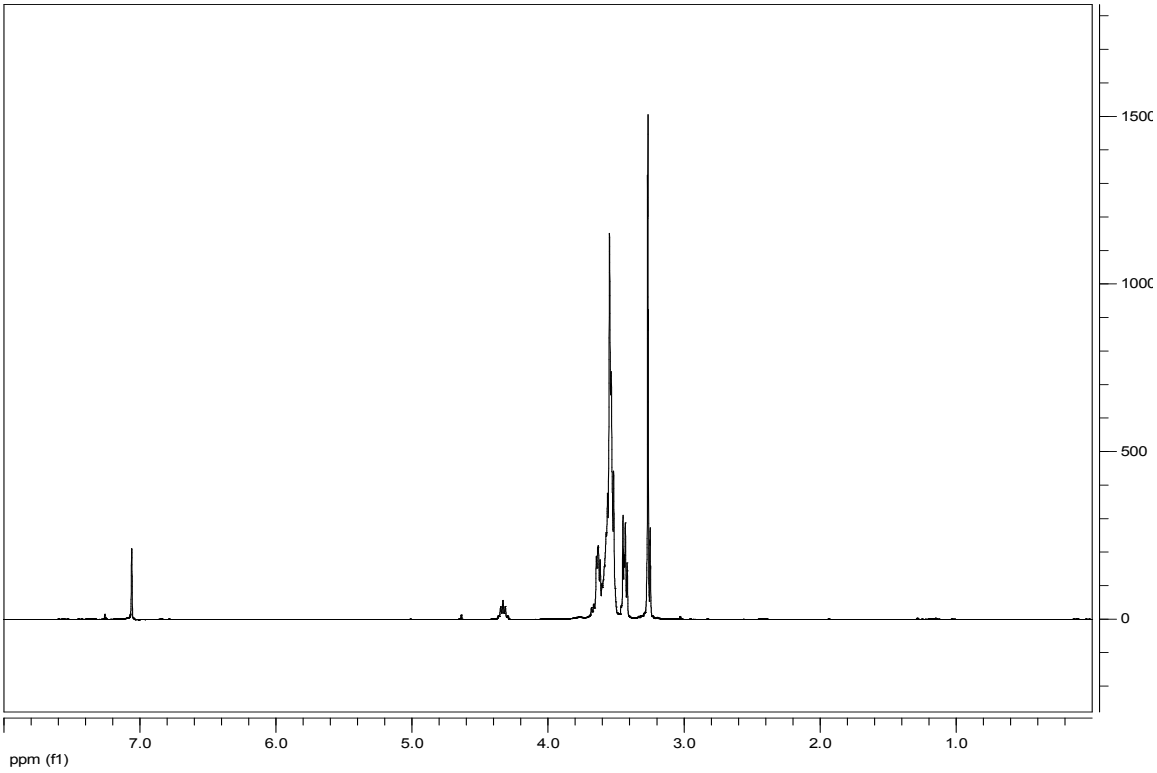

Figure B.11 ^{1}H NMR spectrum of **2.6** in $CDCl_3$

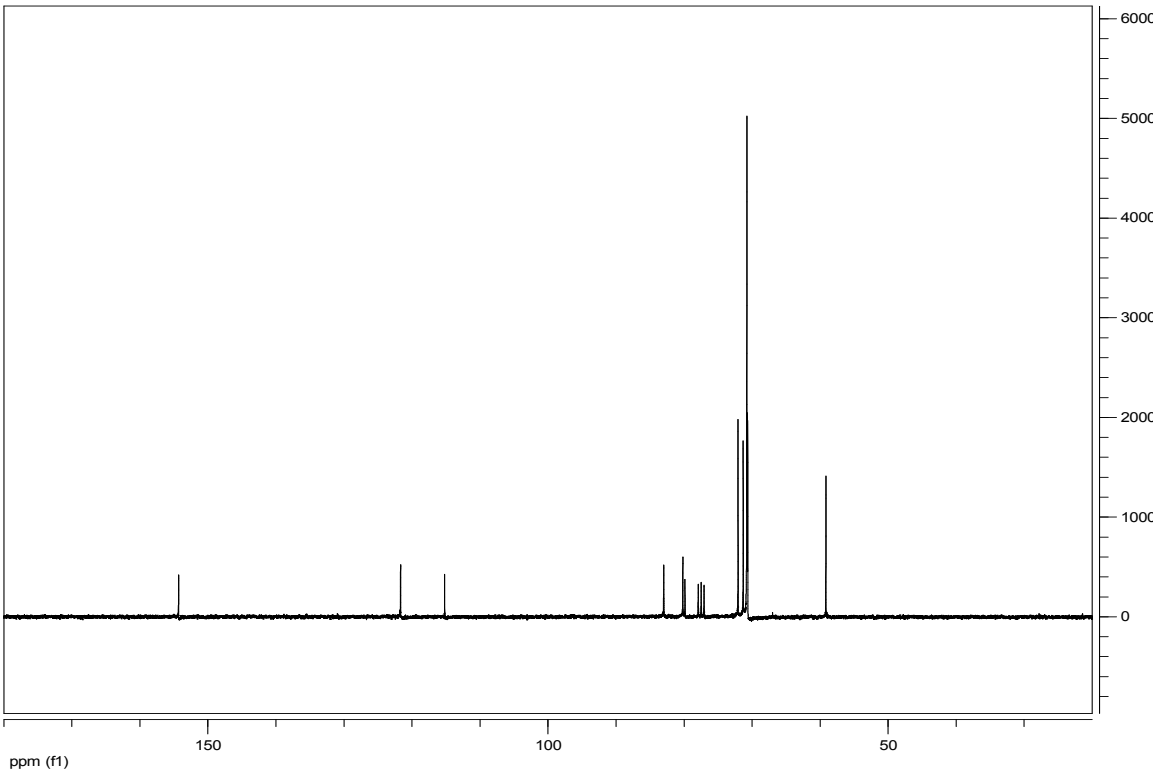

Figure B.12 ^{13}C NMR spectrum of **2.6** in $CDCl_3$

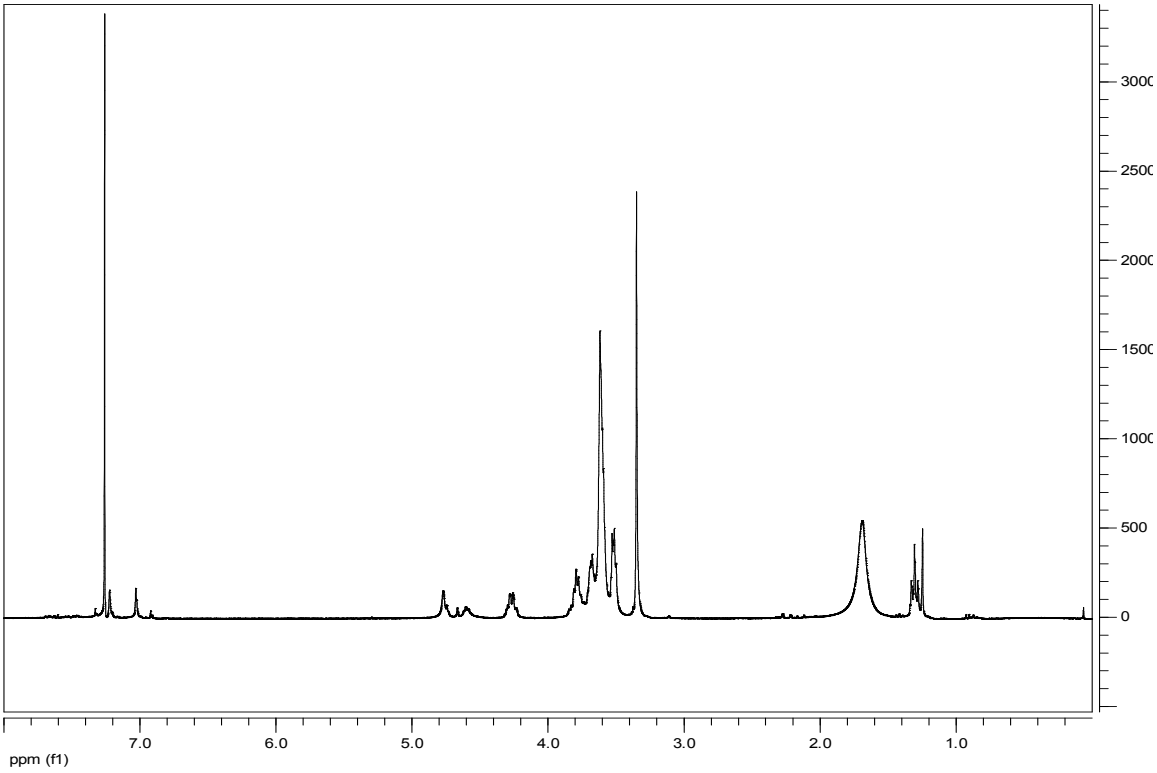

Figure B.13 ^{1}H NMR spectrum of **2.7** in $CDCl_3$

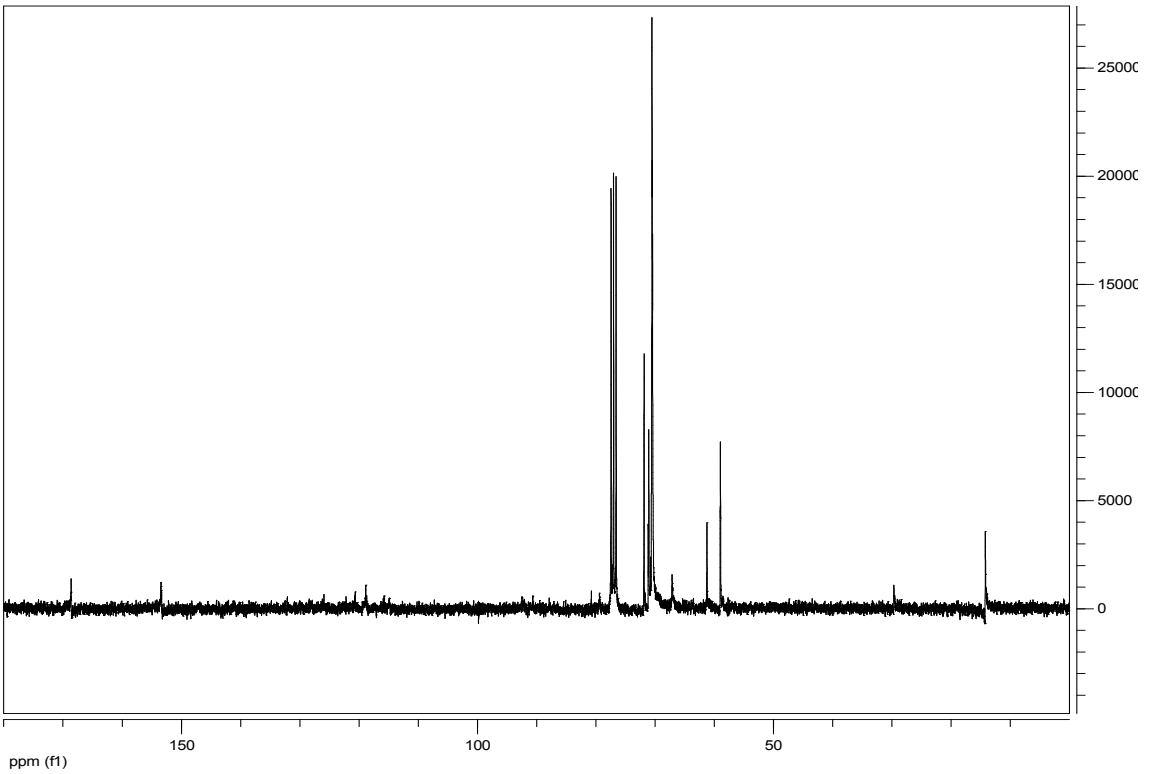

Figure B.14 ^{13}C NMR spectrum of **2.7** in $CDCl_3$

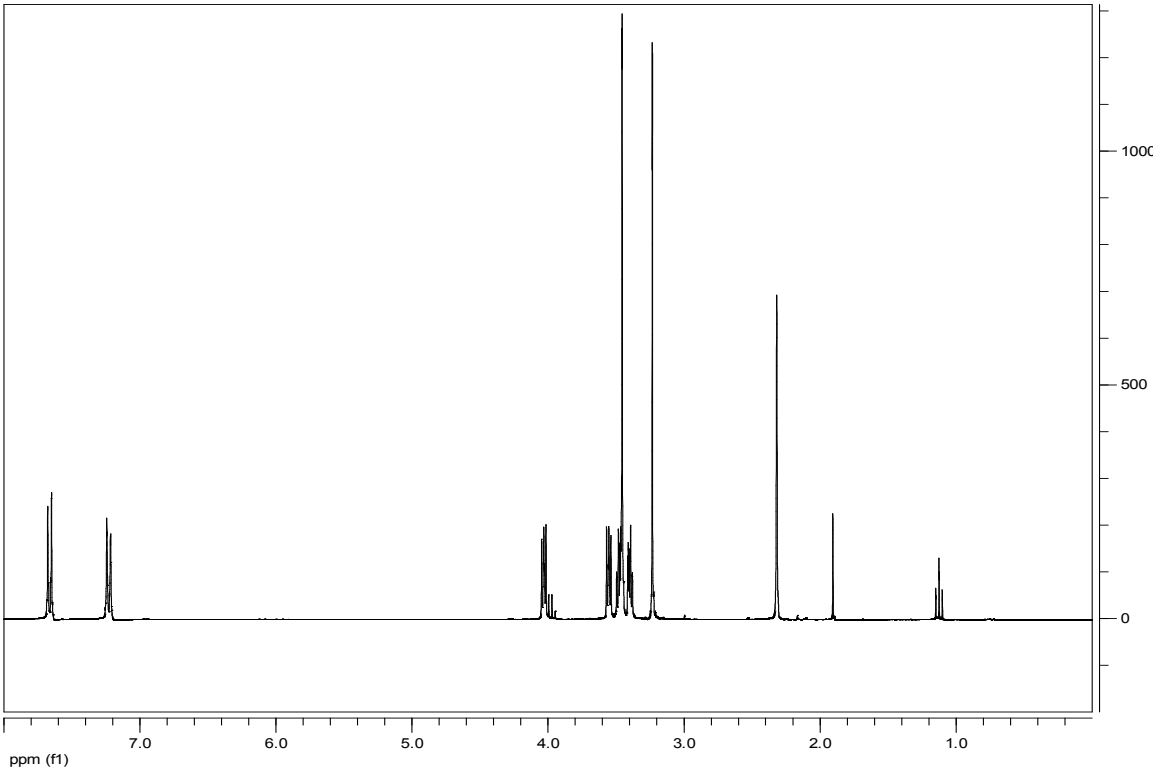

Figure B.15 ^{1}H NMR spectrum of **3.2** in $CDCl_3$

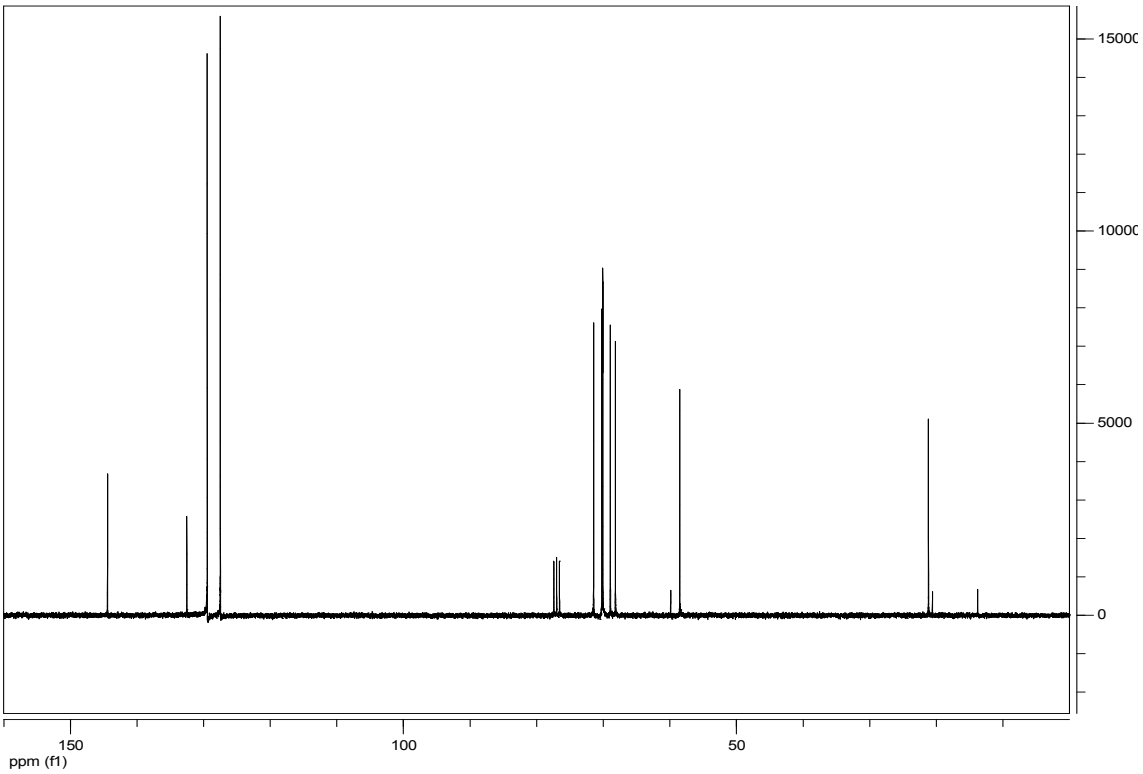

Figure B.16 ^{13}C NMR spectrum of **3.2** in $CDCl_3$

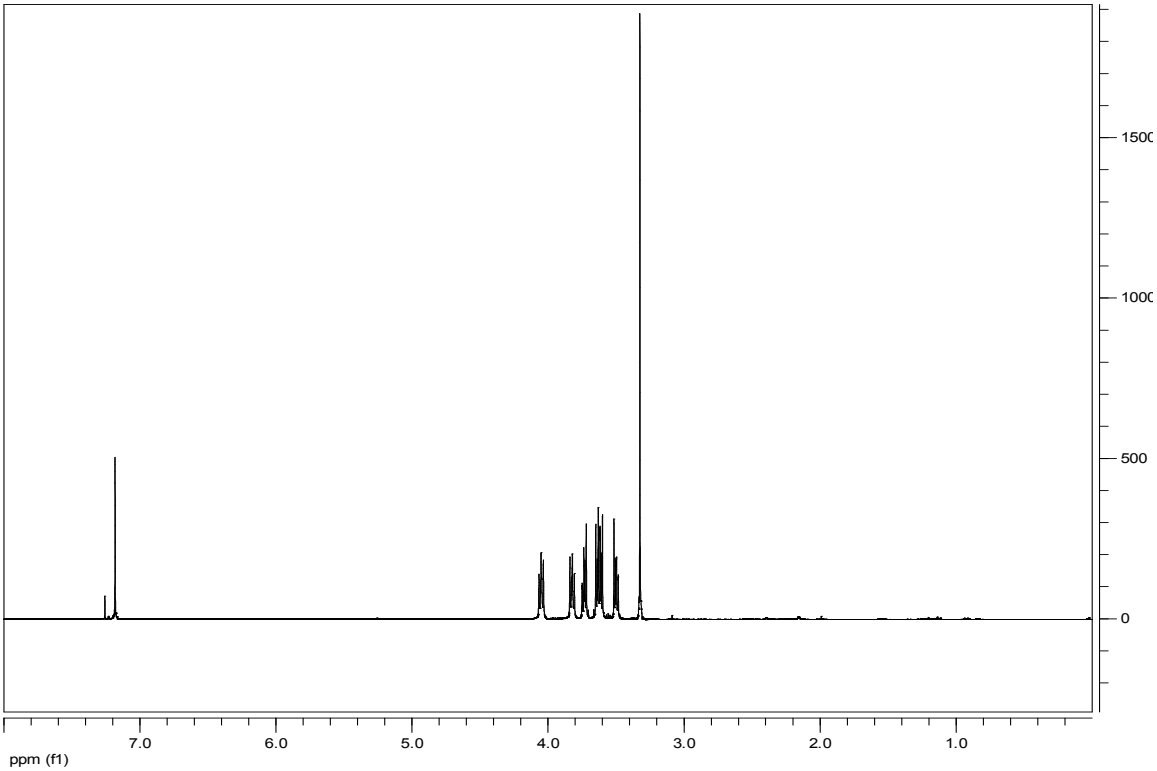

Figure B.17 ^{1}H NMR spectrum of **3.3** in $CDCl_3$

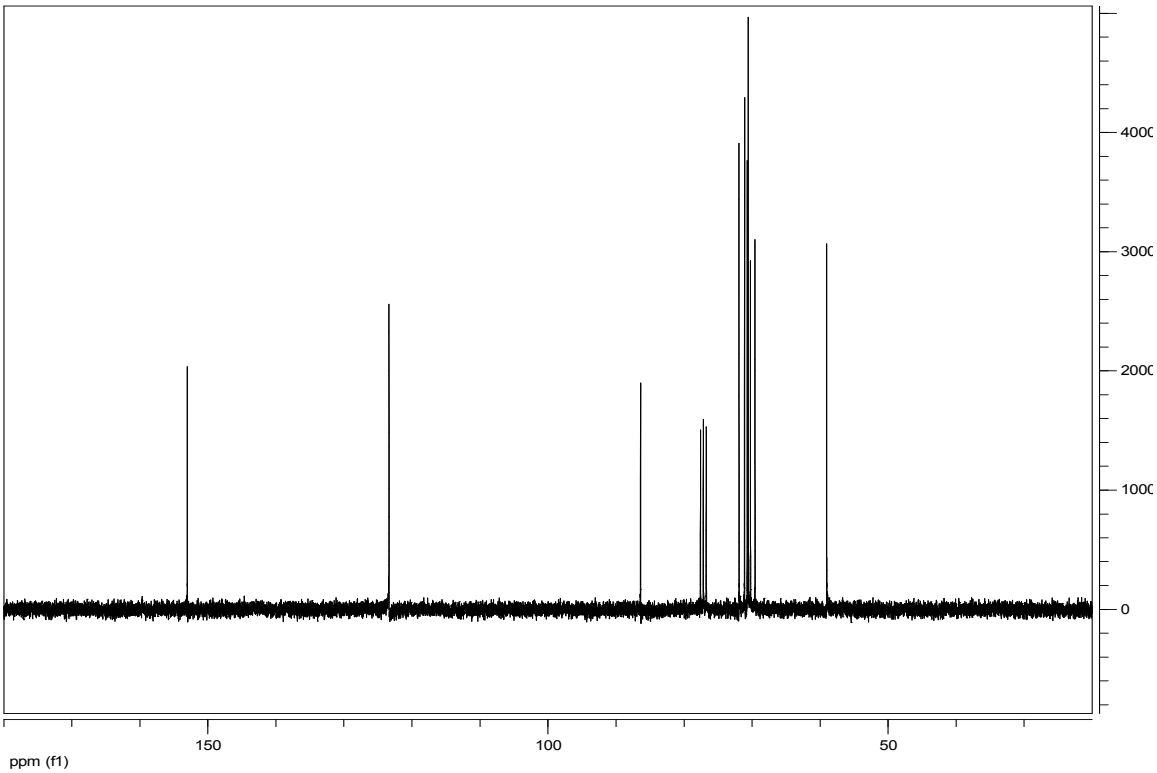

Figure B.18 ^{13}C NMR spectrum of **3.3** in $CDCl_3$

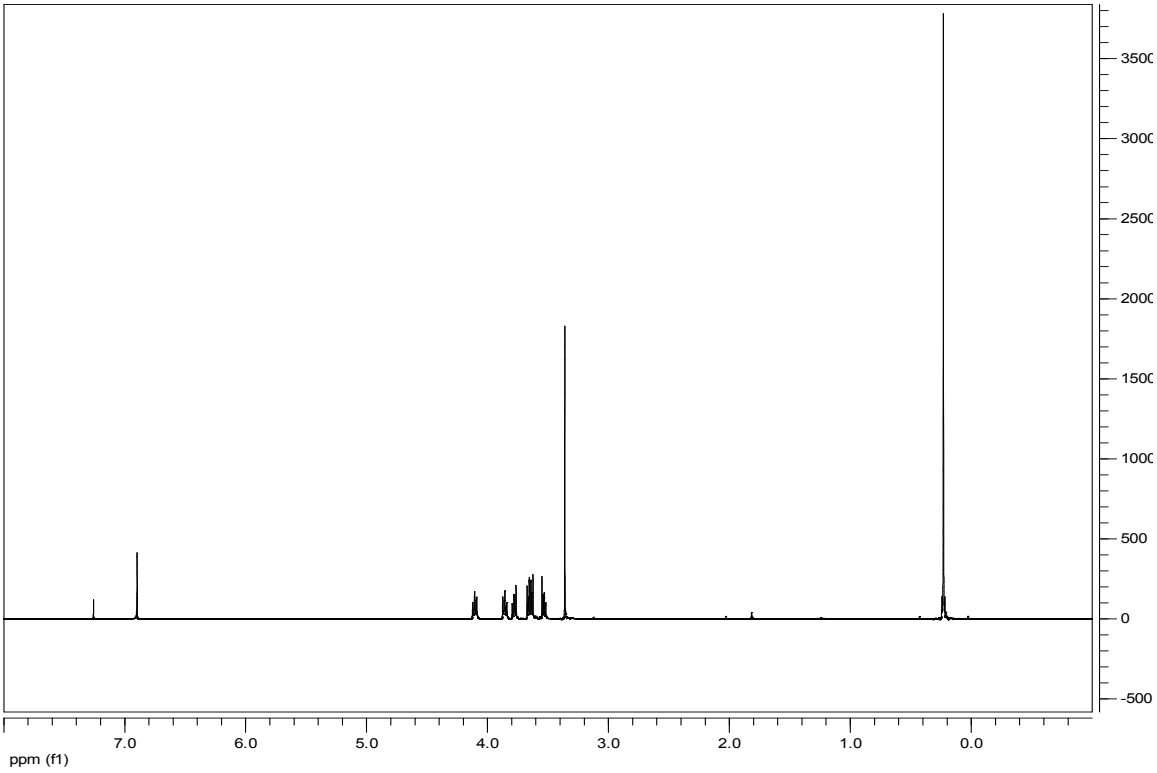

Figure B.19 ^{1}H NMR spectrum of **3.4** in $CDCl_3$

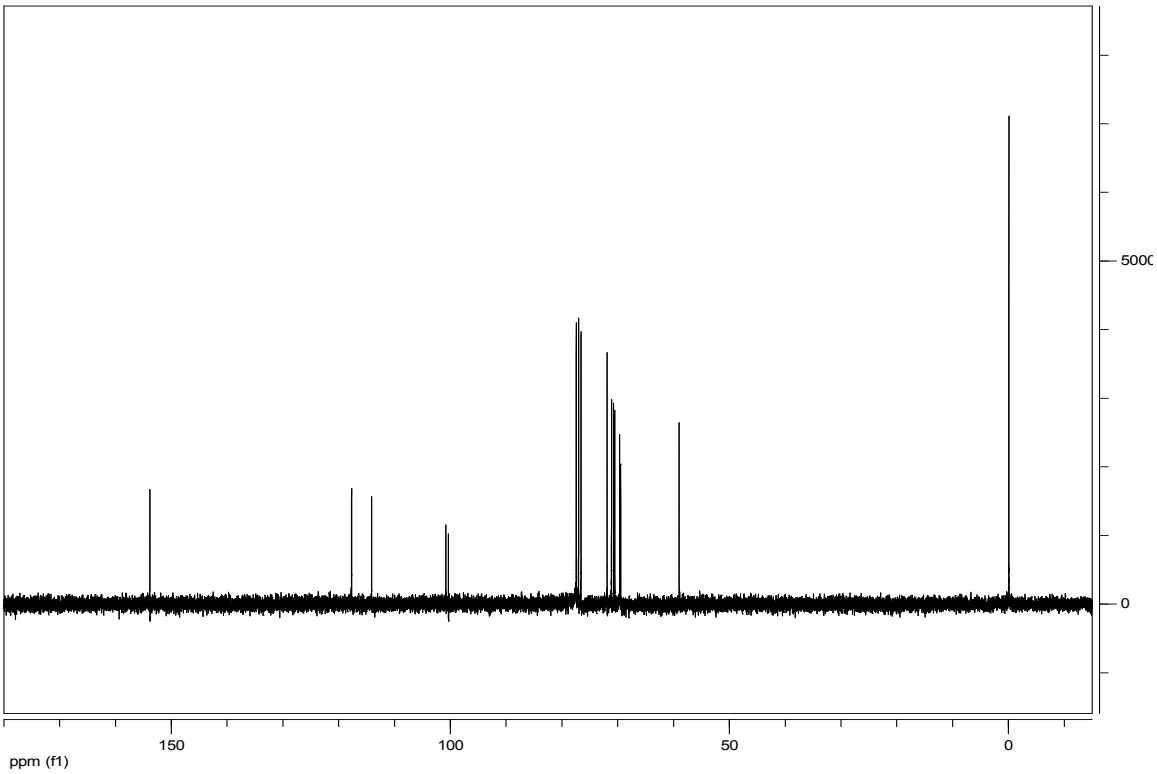

Figure B.20 ^{13}C NMR spectrum of **3.4** in $CDCl_3$

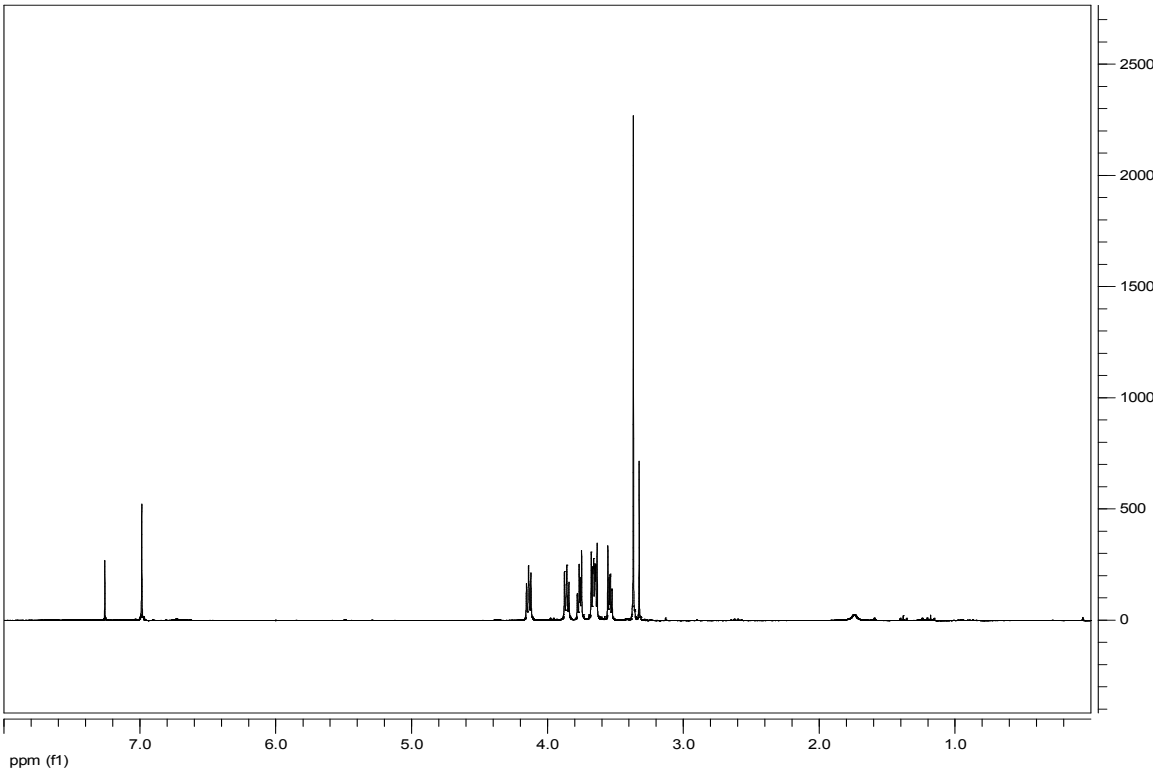

Figure B.21 ^{1}H NMR spectrum of **3.5** in $CDCl_3$

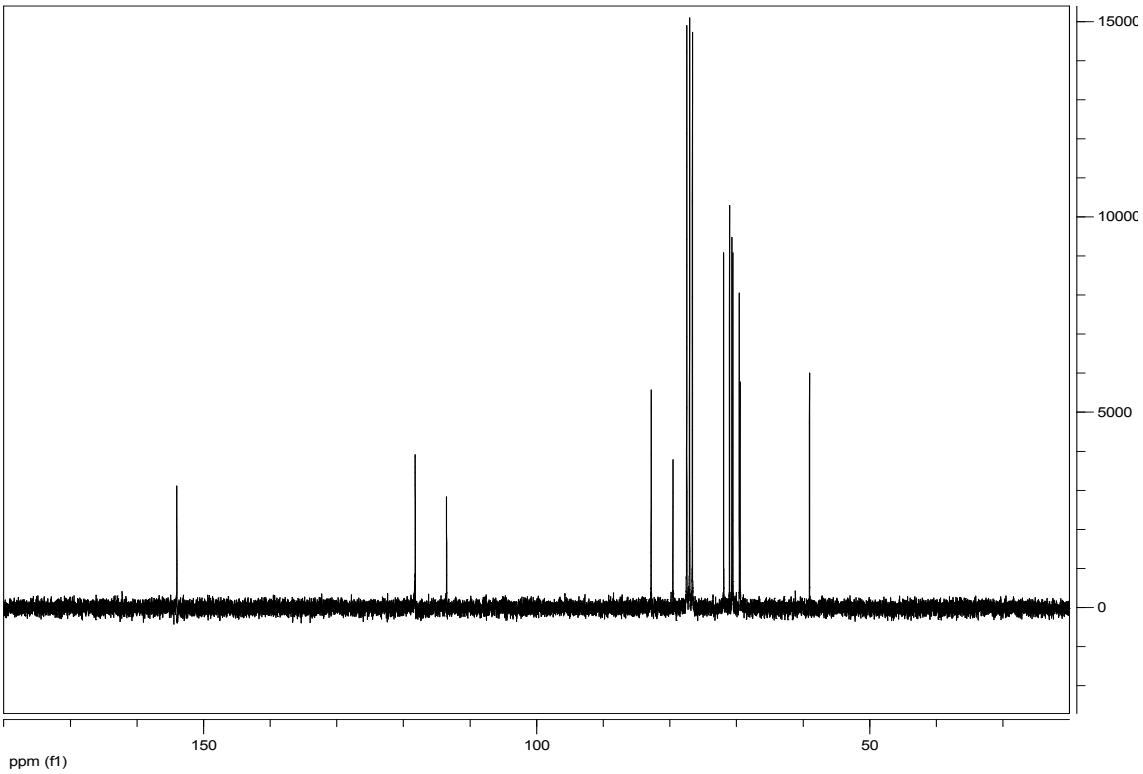

Figure B.22 ^{13}C NMR spectrum of **3.5** in $CDCl_3$

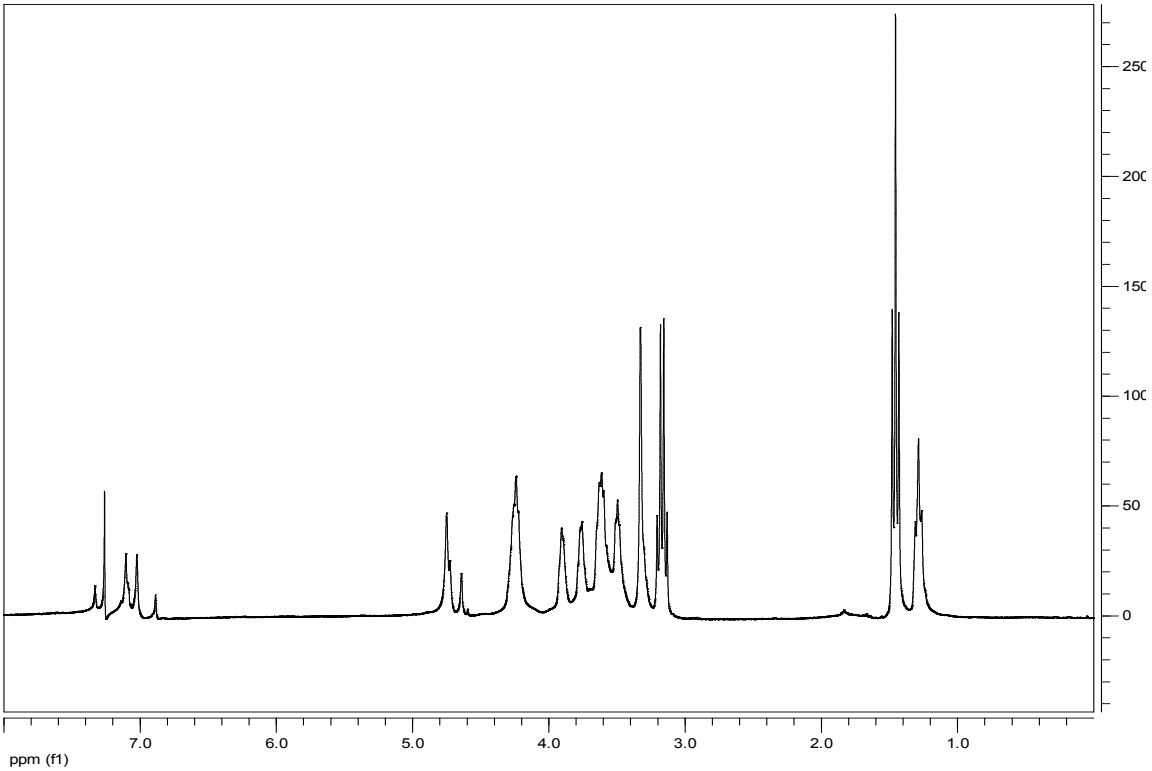

Figure B.23 ^{1}H NMR spectrum of **3.6** in $CDCl_3$

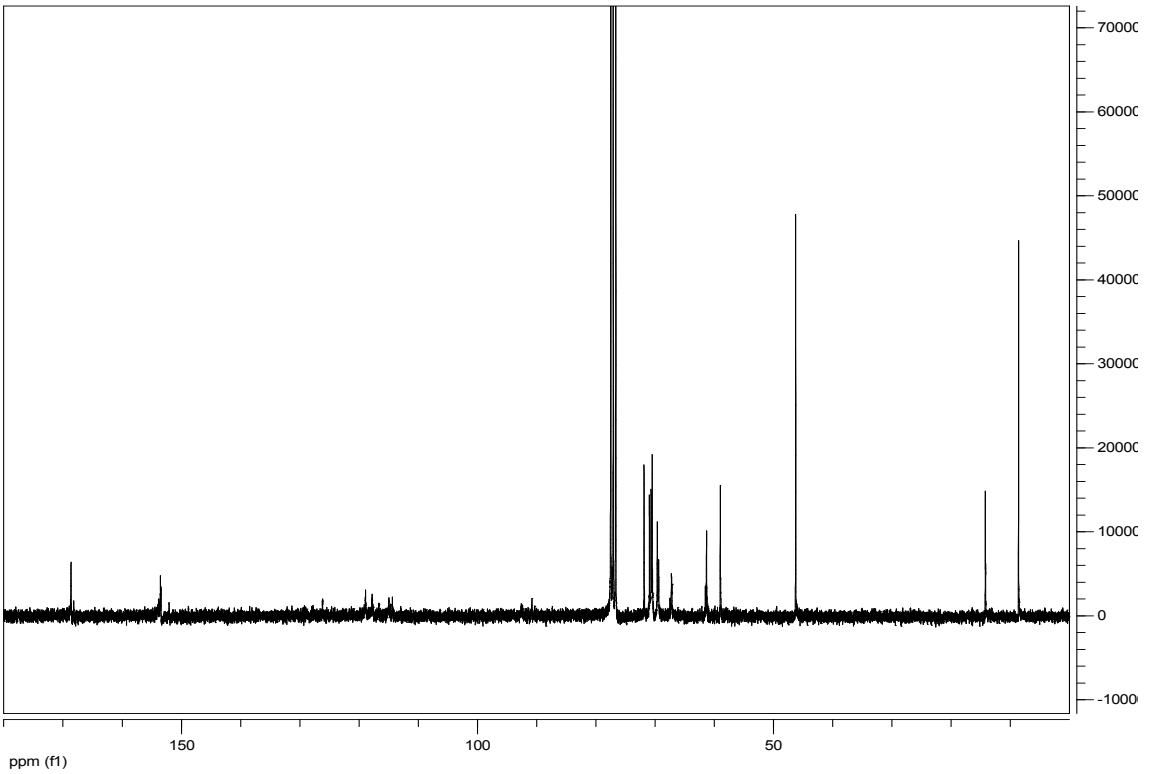

Figure B.24 ^{13}C NMR spectrum of **3.6** in $CDCl_3$

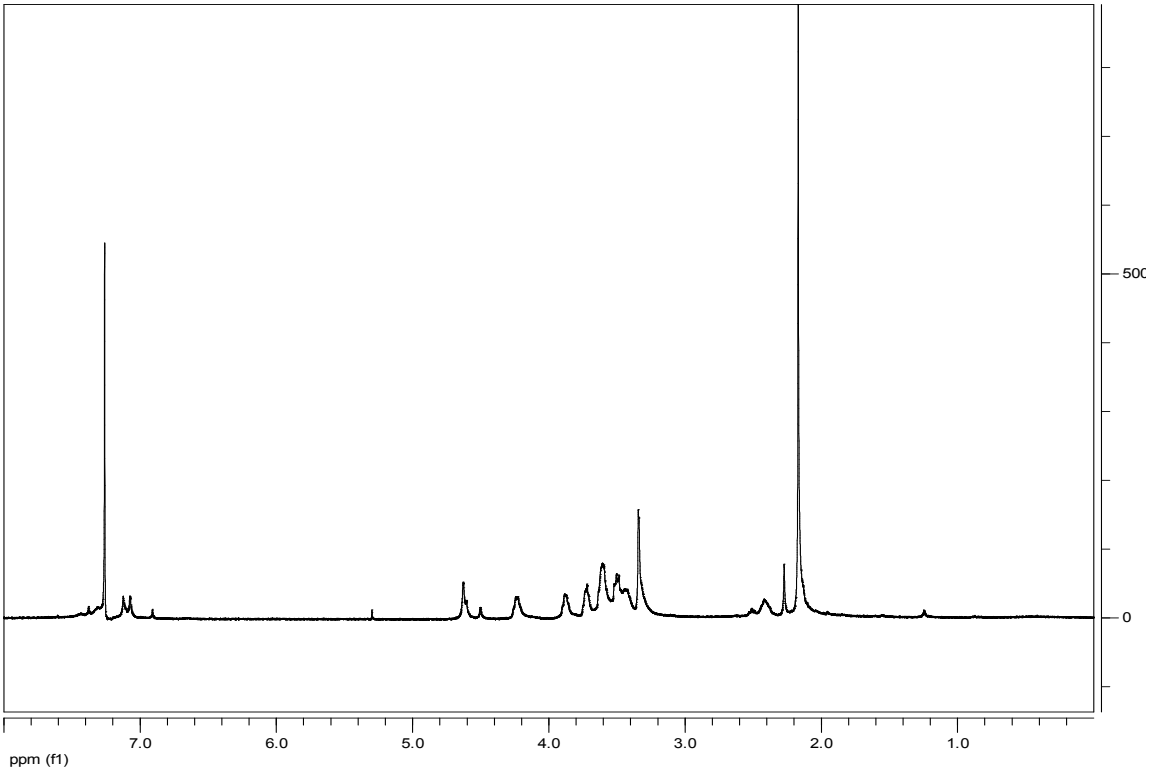

Figure B.25 ^{1}H NMR spectrum of **3.7** in $CDCl_3$

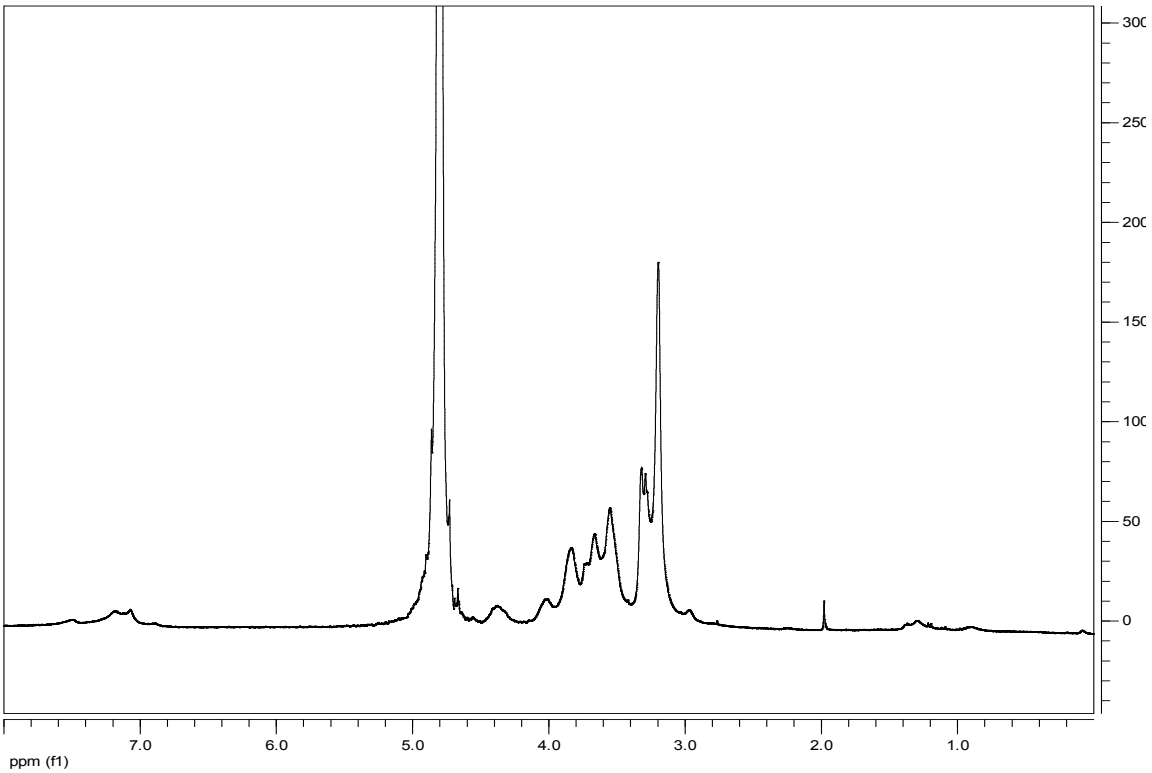

Figure B.26 ^{1}H NMR spectrum of **3** in D_2O

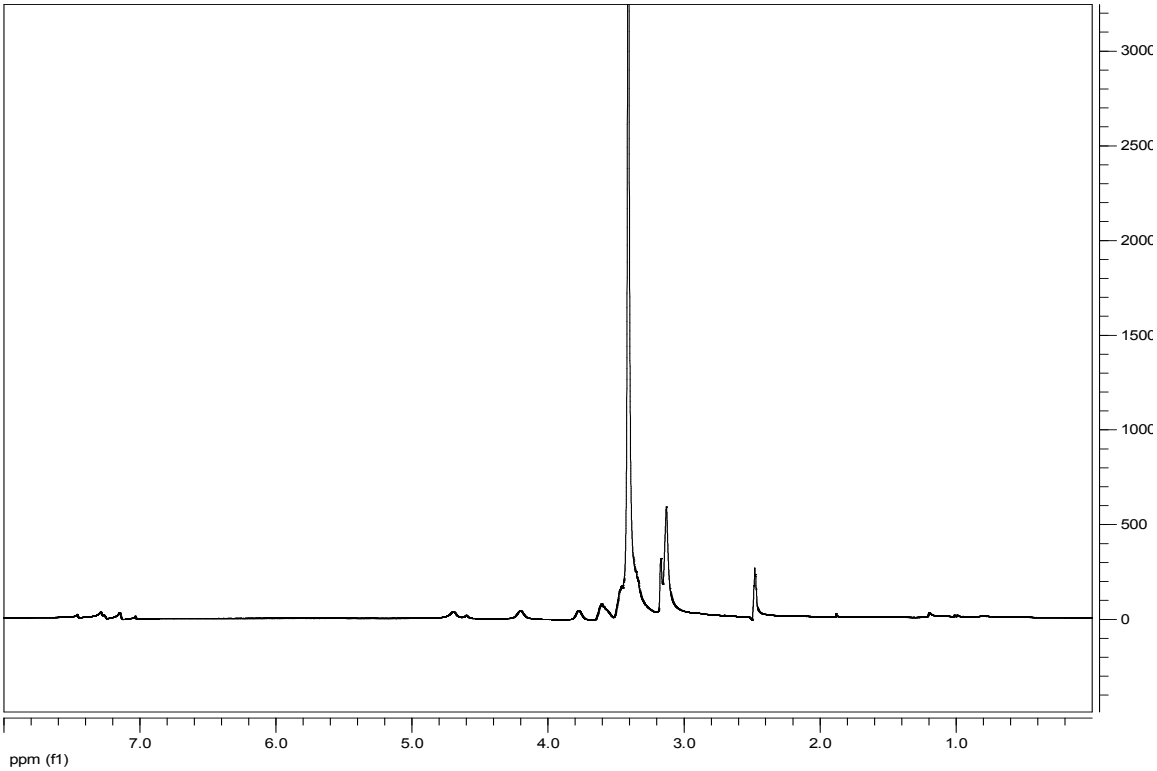

Figure B.27 ^{1}H NMR spectrum of **3** in DMSO

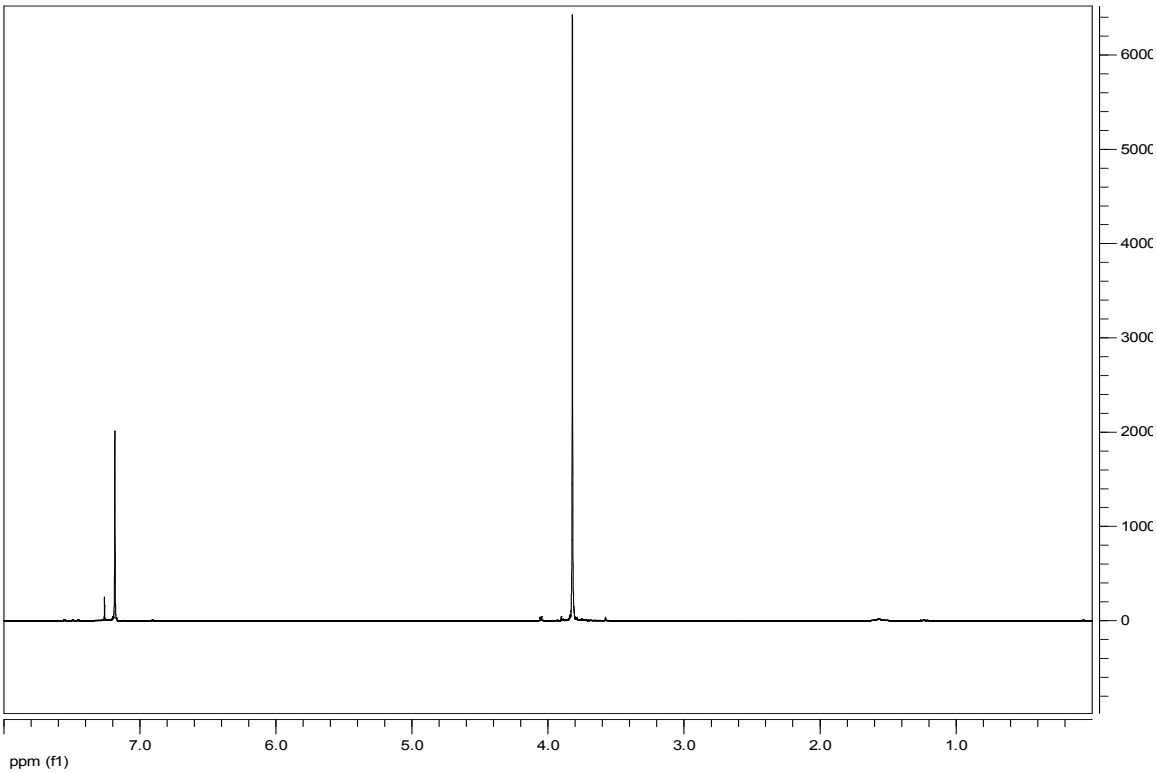

Figure B.28 ^{1}H NMR spectrum of 2,5-diiodo(*p*-dimethoxybenzene) in $CHCl_3$

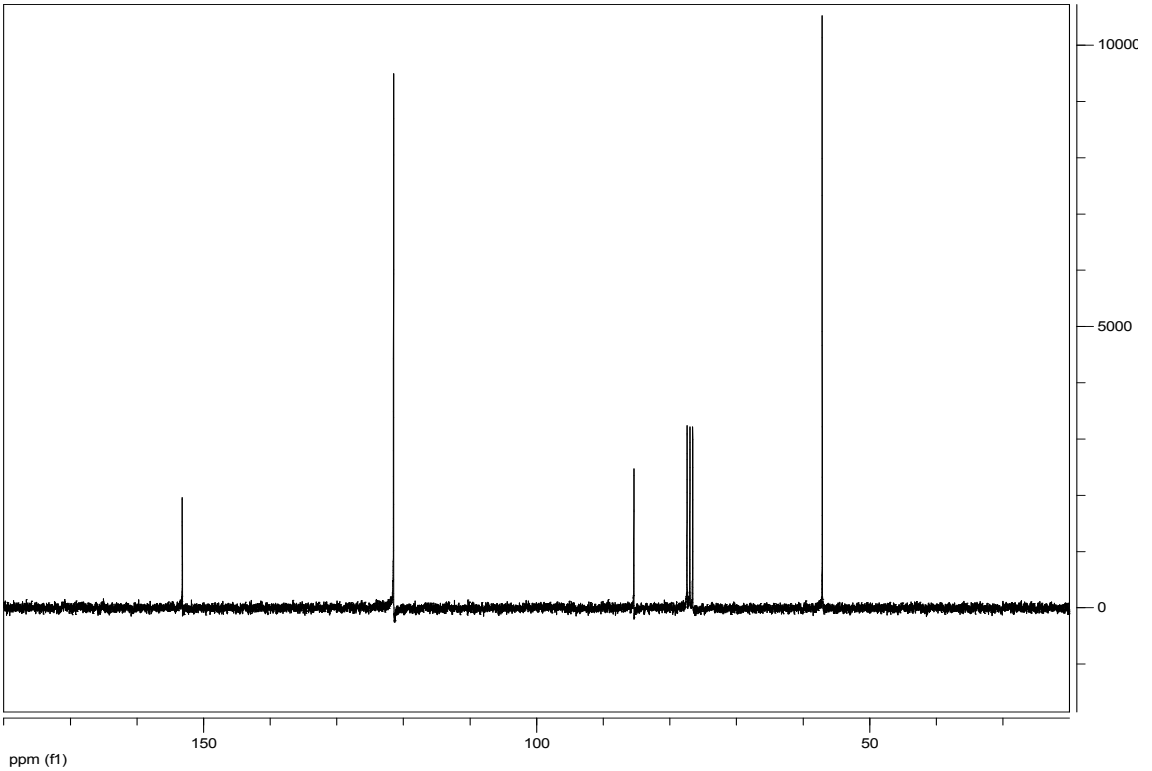

Figure B.29 ^{13}C NMR spectrum of 2,5-diiodo(*p*-dimethoxybenzene) in $CHCl_3$

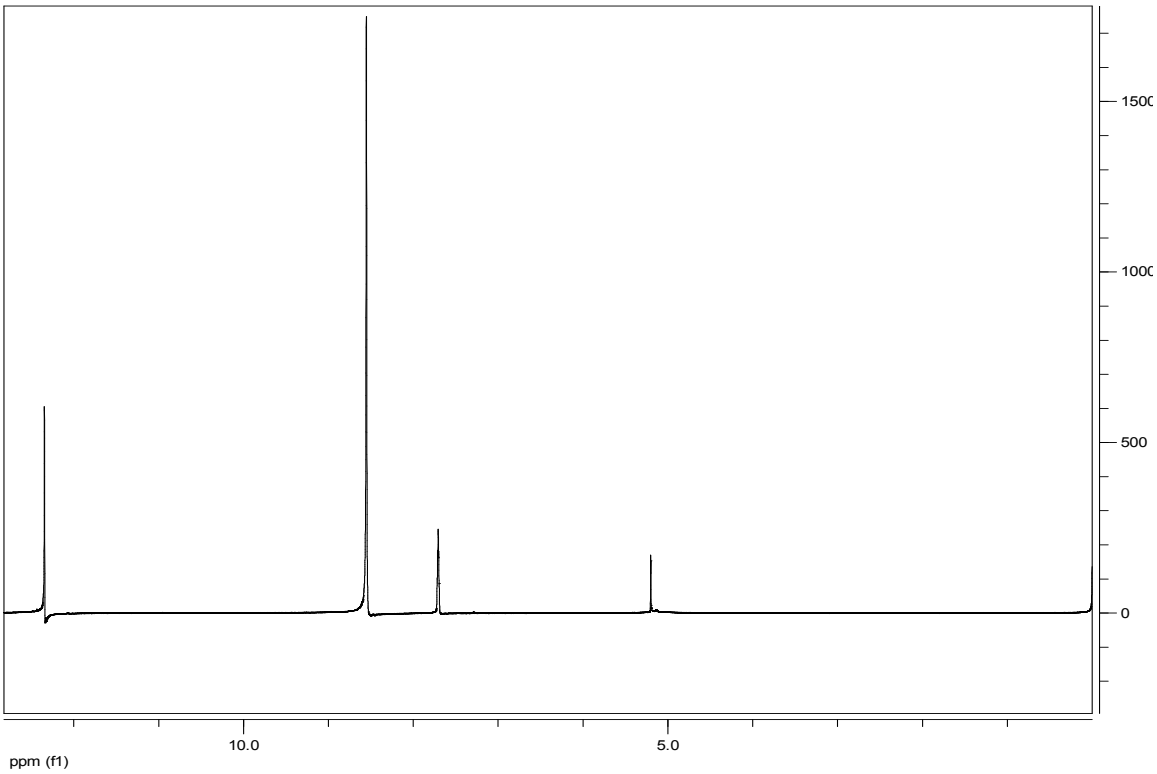

Figure B.30 ^{1}H NMR spectrum of 2,5-diiododihydroquinone in $CHCl_3$

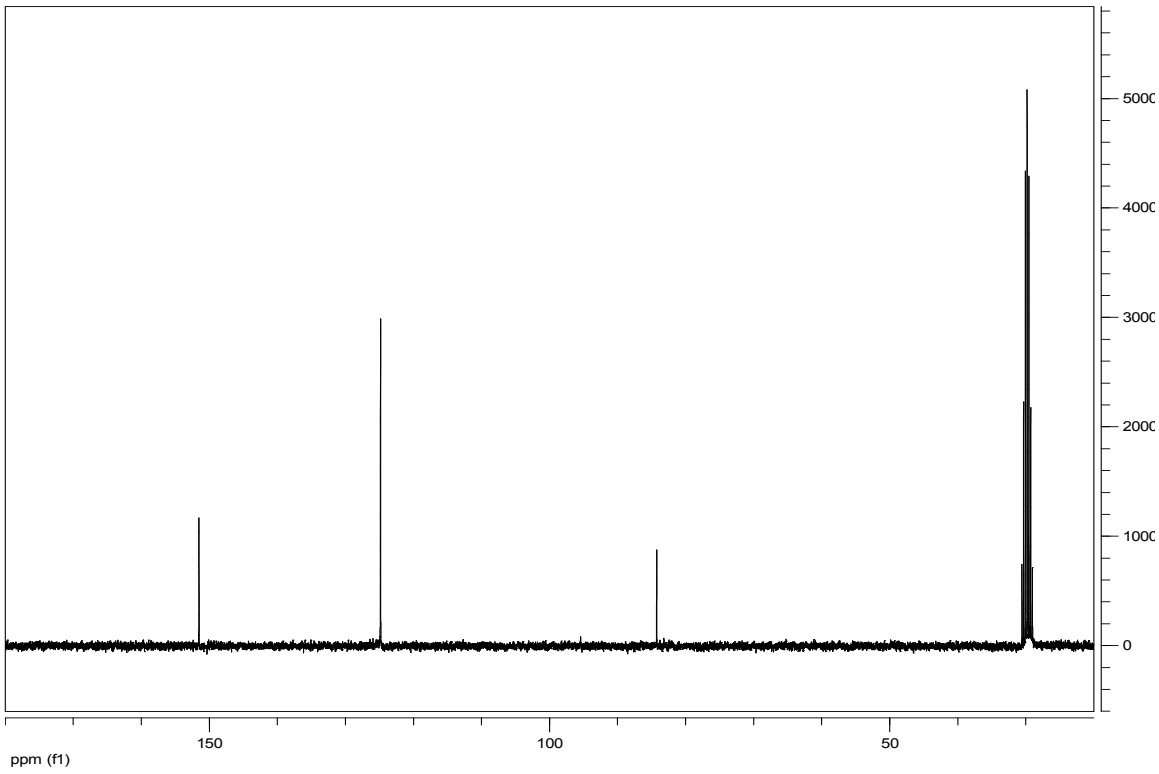

Figure B.31 ^{13}C NMR spectrum of 2,5-diiododihydroquinone in DMSO

REFERENCES

1. (a) Gurunathan, K.; Murugan, A. V.; Marimuthu, R.; Mulik, U. P.; Amalnerkar, D. P., Electrochemically synthesised conducting polymeric materials for applications towards technology in electronics, optoelectronics and energy storage devices. *Materials Chemistry and Physics* **1999,** *61* (3), 173-191; (b) Saxena, V.; Malhotra, B. D., Prospects of conducting polymers in molecular electronics. *Current Applied Physics* **2003,** *3* (2-3), 293-305; (c) Bunz, U. H. F., Poly(aryleneethynylene)s: Syntheses, properties, structures, and applications. *Chemical Reviews* **2000,** *100* (4), 1605-1644.
2. Bunz, U. H. F., Poly(aryleneethynylene)s. *Macromolecular Rapid Communications* **2009,** *30* (9-10), 772-805.
3. Thomas, S. W.; Joly, G. D.; Swager, T. M., Chemical sensors based on amplifying fluorescent conjugated polymers. *Chemical Reviews* **2007,** *107* (4), 1339-1386.
4. Jiang, H.; Taranekar, P.; Reynolds, J. R.; Schanze, K. S., Conjugated Polyelectrolytes: Synthesis, Photophysics, and Applications. *Angewandte Chemie-International Edition* **2009,** *48* (24), 4300-4316.
5. (a) Chen, L. H.; McBranch, D. W.; Wang, H. L.; Helgeson, R.; Wudl, F.; Whitten, D. G., Highly sensitive biological and chemical sensors based on reversible fluorescence quenching in a conjugated polymer. *Proceedings of the National Academy of Sciences of the United States of America* **1999,** *96* (22), 12287-12292; (b) McQuade, D. T.; Pullen, A. E.; Swager, T. M., Conjugated polymer-based chemical sensors. *Chemical Reviews* **2000,** *100* (7), 2537-2574.
6. (a) Yang, J. S.; Swager, T. M., Fluorescent porous polymer films as TNT chemosensors: Electronic and structural effects. *Journal of the American Chemical Society* **1998,** *120* (46), 11864-11873; (b) Cumming, C. J.; Aker, C.; Fisher, M.; Fox, M.; la Grone, M. J.; Reust, D.; Rockley, M. G.; Swager, T. M.; Towers, E.; Williams, V., Using novel fluorescent polymers as sensory materials for above-ground sensing of chemical signature compounds emanating from buried landmines. *Ieee Transactions on Geoscience and Remote Sensing* **2001,** *39* (6), 1119-1128.
7. Vaddiraju, S.; Gleason, K. K., Selective sensing of volatile organic compounds using novel conducting polymer-metal nanoparticle hybrids. *Nanotechnology* **2010,** *21* (12).
8. Liu, B.; Yu, W. L.; Pei, J.; Liu, S. Y.; Lai, Y. H.; Huang, W., Design and synthesis of bipyridyl-containing conjugated polymers: Effects of polymer rigidity on metal ion sensing. *Macromolecules* **2001,** *34* (23), 7932-7940.
9. Reppy, M. A.; Pindzola, B. A., Biosensing with polydiacetylene materials: structures, optical properties and applications. *Chemical Communications* **2007,** (42), 4317-4338.
10. (a) Gaylord, B. S.; Heeger, A. J.; Bazan, G. C., DNA detection using water-soluble conjugated polymers and peptide nucleic acid probes. *Proceedings of the National Academy of Sciences of the United States of America* **2002,** *99* (17), 10954-10957; (b) Gaylord, B. S.; Heeger, A. J.; Bazan, G. C., DNA hybridization detection with water-soluble conjugated polymers and chromophore-labeled single-stranded DNA. *Journal of the American Chemical Society* **2003,** *125* (4), 896-900.

11. (a) Li, K.; Liu, B., Water-soluble conjugated polymers as the platform for protein sensors. *Polymer Chemistry* **2010,** *1* (3), 252-259; (b) Yu, D. Y.; Zhang, Y.; Liu, B., Interpolyelectrolyte complexes of anionic water-soluble conjugated polymers and proteins as platforms for multicolor protein sensing and quantification. *Macromolecules* **2008,** *41* (11), 4003-4011.
12. Disney, M. D.; Zheng, J.; Swager, T. M.; Seeberger, P. H., Detection of bacteria with carbohydrate-functionalized fluorescent polymers. *Journal of the American Chemical Society* **2004,** *126* (41), 13343-13346.
13. Xue, C. H.; Luo, F. T.; Chen, J.; Liu, H. Y., Synthesis and biosensing application of highly water-soluble and cross-linkable poly(p-phenyleneethynylene) containing osmium(II) complex and aldehyde groups. *Analytica Chimica Acta* **2006,** *569* (1-2), 27-34.
14. Zhao, X. Y.; Liu, Y.; Schanze, K. S., A conjugated polyelectrolyte-based fluorescence sensor for pyrophosphate. *Chemical Communications* **2007,** (28), 2914-2916.
15. Fan, C. H.; Plaxco, K. W.; Heeger, A. J., High-efficiency fluorescence quenching of conjugated polymers by proteins. *Journal of the American Chemical Society* **2002,** *124* (20), 5642-5643.
16. Liu, M.; Kaur, P.; Waldeck, D. H.; Xue, C. H.; Liu, H. Y., Fluorescence quenching mechanism of a polyphenylene polyelectrolyte with other macromolecules: Cytochrome c and dendrimers. *Langmuir* **2005,** *21* (5), 1687-1690.
17. Bunz, U. H. F.; Rotello, V. M., Gold Nanoparticle-Fluorophore Complexes: Sensitive and Discerning "Noses" for Biosystems Sensing. *Angewandte Chemie-International Edition* **2010,** *49* (19), 3268-3279.
18. Albert, K. J.; Lewis, N. S.; Schauer, C. L.; Sotzing, G. A.; Stitzel, S. E.; Vaid, T. P.; Walt, D. R., Cross-reactive chemical sensor arrays. *Chemical Reviews* **2000,** *100* (7), 2595-2626.
19. (a) Phillips, R. L.; Kim, I. B.; Carson, B. E.; Tidbeck, B.; Bai, Y.; Lowary, T. L.; Tolbert, L. M.; Bunz, U. H. F., Sugar-Substituted Poly(p-phenyleneethynylene)s: Sensitivity Enhancement toward Lectins and Bacteria. *Macromolecules* **2008,** *41* (20), 7316-7320; (b) Li, C. H.; Zhou, C. J.; Zheng, H. Y.; Yin, X. D.; Zuo, Z. C.; Liu, H. B.; Li, Y. L., Synthesis of a novel poly(para-phenylene ethynylene)for highly selective and sensitive sensing mercury (II) ions. *Journal of Polymer Science Part a-Polymer Chemistry* **2008,** *46* (6), 1998-2007.
20. Khan, A.; Muller, S.; Hecht, S., Practical synthesis of an amphiphilic, non-ionic poly(paraphenyleneethynylene) derivative with a remarkable quantum yield in water. *Chemical Communications* **2005,** (5), 584-586.
21. (a) Wilson, J. N.; Windscheif, P. M.; Evans, U.; Myrick, M. L.; Bunz, U. H. F., Band gap engineering of poly(p-phenyleneethynylene)s: Cross-conjugated PPE-PPV hybrids. *Macromolecules* **2002,** *35* (23), 8681-8683; (b) Kim, I. B.; Phillips, R.; Bunz, U. H. F., Carboxylate group side-chain density modulates the pH-dependent optical properties of PPEs. *Macromolecules* **2007,** *40* (15), 5290-5293.
22. (a) Kim, I. B.; Bunz, U. H. F., Modulating the sensory response of a conjugated polymer by proteins: An agglutination assay for mercury ions in water. *Journal of the American Chemical Society* **2006,** *128* (9), 2818-2819; (b) Kim, I. B.; Phillips, R.; Bunz,

U. H. F., Forced agglutination as a tool to improve the sensory response of a carboxylated poly(p-phenyleneethynylene). *Macromolecules* **2007,** *40* (4), 814-817.
23. (a) Kim, I. B.; Dunkhorst, A.; Gilbert, J.; Bunz, U. H. F., Sensing of lead ions by a carboxylate-substituted PPE: Multivalency effects. *Macromolecules* **2005,** *38* (11), 4560-4562; (b) Kim, I. B.; Erdogan, B.; Wilson, J. N.; Bunz, U. H. F., Sugar-poly(para-phenylene ethynylene) conjugates as sensory materials: Efficient quenching by Hg^{2+} and Pb^{2+} ions. *Chemistry-a European Journal* **2004,** *10* (24), 6247-6254.
24. Kim, I. B.; Shin, H.; Garcia, A. J.; Bunz, U. H. F., Use of a folate-PPE conjugate to image cancer cells in vitro. *Bioconjugate Chemistry* **2007,** *18* (3), 815-820.
25. Phillips, R. L.; Miranda, O. R.; You, C. C.; Rotello, V. M.; Bunz, U. H. F., Rapid and efficient identification of bacteria using gold-nanoparticle - Poly(para-phenyleneethynylene) constructs. *Angewandte Chemie-International Edition* **2008,** *47* (14), 2590-2594.
26. Miranda, O. R.; You, C. C.; Phillips, R.; Kim, I. B.; Ghosh, P. S.; Bunz, U. H. F.; Rotello, V. M., Array-based sensing of proteins using conjugated polymers. *Journal of the American Chemical Society* **2007,** *129* (32), 9856-9857.
27. Zheng, J.; Swager, T. M., Poly(arylene ethynylene)s in Chemosensing and Biosensing. In *Poly(Arylene Etynylene)S: From Synthesis to Application*, 2005; Vol. 177, pp 151-179.
28. (a) Tan, C. Y.; Pinto, M. R.; Schanze, K. S., Photophysics, aggregation and amplified quenching of a water-soluble poly(phenylene ethynylene). *Chemical Communications* **2002,** (5), 446-447; (b) Pinto, M. R.; Kristal, B. M.; Schanze, K. S., A water-soluble poly(phenylene ethynylene) with pendant phosphonate groups. Synthesis, photophysics, and layer-by-layer self-assembled films. *Langmuir* **2003,** *19* (16), 6523-6533; (c) Pinto, M. R.; Schanze, K. S., Conjugated polyelectrolytes: Synthesis and applications. *Synthesis-Stuttgart* **2002,** (9), 1293-1309.
29. Bao, B. Q.; Yuwen, L.; Zhan, X. W.; Wang, L. H., Water-Soluble Hyperbranched Polyelectrolytes with High Fluorescence Quantum Yield: Facile Synthesis and Selective Chemosensor for Hg2+ and Cu2+ Ions. *Journal of Polymer Science Part a-Polymer Chemistry* **2010,** *48* (15), 3431-3439.
30. Zhu, B.; Han, Y.; Sun, M. H.; Bo, Z. S., Water-soluble dendronized polyfluorenes with an extremely high quantum yield in water. *Macromolecules* **2007,** *40* (13), 4494-4500.
31. Hakomori, S., Glycosylation defining cancer malignancy: New wine in an old bottle. *Proceedings of the National Academy of Sciences of the United States of America* **2002,** *99* (16), 10231-10233.
32. Meezan, E.; Wu, H. C.; Black, P. H.; Robbins, P. W., Comparative Studies on Carbohydrate-containing Membrane Components of Normal and Virus-transformed Mouse Fibroblasts .2. Separation of Gylcoproteins and Glycopeptides by Sephadex Chromatography. *Biochemistry* **1969,** *8* (6), 2518-&.
33. Dube, D. H.; Bertozzi, C. R., Glycans in cancer and inflammation. Potential for therapeutics and diagnostics. *Nature Reviews Drug Discovery* **2005,** *4* (6), 477-488.
34. Fuster, M. M.; Esko, J. D., The sweet and sour of cancer: Glycans as novel therapeutic targets. *Nature Reviews Cancer* **2005,** *5*, 526-542.
35. Bajaj, A.; Miranda, O. R.; Kim, I. B.; Phillips, R. L.; Jerry, D. J.; Bunz, U. H. F.; Rotello, V. M., Detection and differentiation of normal, cancerous, and metastatic cells

using nanoparticle-polymer sensor arrays. *Proceedings of the National Academy of Sciences of the United States of America* **2009,** *106* (27), 10912-10916.
36. (a) Perez, J. B.; Martinez, K. L.; Segura, J. M.; Vogel, H., Supported cell-membrane sheets for functional fluorescence imaging of membrane proteins. *Advanced Functional Materials* **2006,** *16* (2), 306-312; (b) Qu, X. C.; Wang, J.; Zhang, Z. X.; Koop, N.; Rahmanzadeh, R.; Huttmann, G., Imaging of cancer cells by multiphoton microscopy using gold nanoparticles and fluorescent dyes. *Journal of Biomedical Optics* **2008,** *13* (3).
37. Zucchero, A. J.; Wilson, J. N.; Bunz, U. H. F., Cruciforms as functional fluorophores: Response to protons and selected metal ions. *Journal of the American Chemical Society* **2006,** *128* (36), 11872-11881.
38. (a) Uechi, I.; Yamada, S., Photochemical and analytical applications of gold nanoparticles and nanorods utilizing surface plasmon resonance. *Analytical and Bioanalytical Chemistry* **2008,** *391* (7), 2411-2421; (b) Rosi, N. L.; Mirkin, C. A., Nanostructures in biodiagnostics. *Chemical Reviews* **2005,** *105* (4), 1547-1562; (c) Mirkin, C. A.; Letsinger, R. L.; Mucic, R. C.; Storhoff, J. J., A DNA-based method for rationally assembling nanoparticles into macroscopic materials. *Nature* **1996,** *382* (6592), 607-609; (d) Elghanian, R.; Storhoff, J. J.; Mucic, R. C.; Letsinger, R. L.; Mirkin, C. A., Selective colorimetric detection of polynucleotides based on the distance-dependent optical properties of gold nanoparticles. *Science* **1997,** *277* (5329), 1078-1081.
39. Lombardi, J. R.; Birke, R. L., A Unified View of Surface-Enhanced Raman Scattering. *Accounts of Chemical Research* **2009,** *42* (6), 734-742.
40. (a) Hutter, E.; Fendler, J. H., Exploitation of localized surface plasmon resonance. *Advanced Materials* **2004,** *16* (19), 1685-1706; (b) Link, S.; El-Sayed, M. A., Shape and size dependence of radiative, non-radiative and photothermal properties of gold nanocrystals. *International Reviews in Physical Chemistry* **2000,** *19* (3), 409-453.
41. (a) Giorgetti, E.; Margheri, G.; Sottini, S.; Muniz-Miranda, A., Investigation of non-linear optical effects at conjugated polymer/silver interface by surface plasmon resonance and surface enhanced Raman scattering. *Synthetic Metals* **2003,** *139* (3), 929-932; (b) Kulkarni, A. P.; Noone, K. M.; Munechika, K.; Guyer, S. R.; Ginger, D. S., Plasmon-Enhanced Charge Carrier Generation in Organic Photovoltaic Films Using Silver Nanoprisms. *Nano Letters* **2010,** *10* (4), 1501-1505.
42. Mahmoud, M. A.; Poncheri, A. J.; Phillips, R. L.; El-Sayed, M. A., Plasmonic Field Enhancement of the Exciton-Exciton Annihilation Process in a Poly(p-phenyleneethynylene) Fluorescent Polymer by Ag Nanocubes. *Journal of the American Chemical Society* **2010,** *132* (8), 2633-2641.